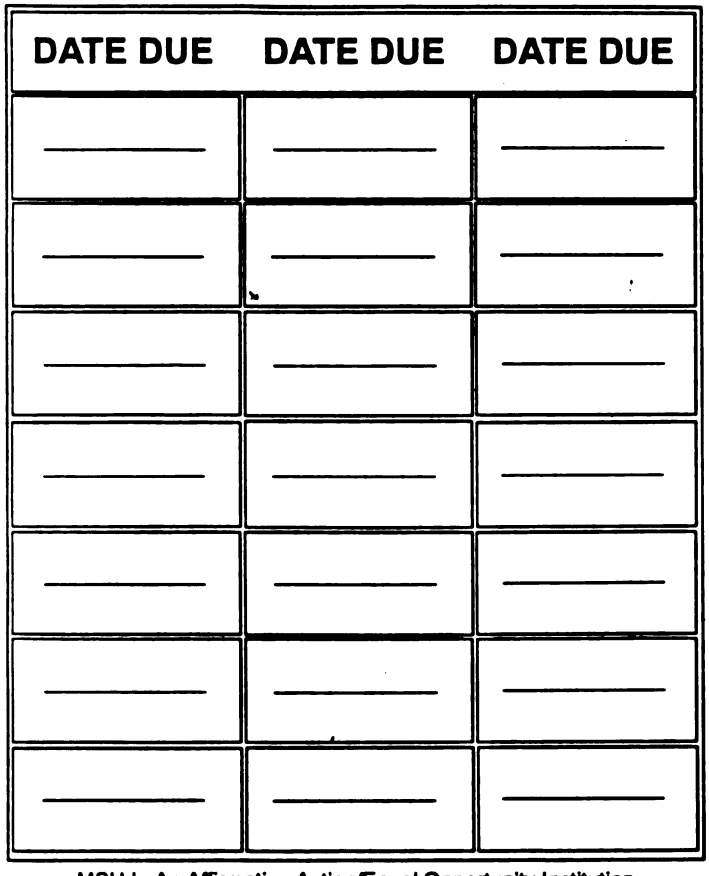

MRI AND CT ANALYSIS OF

OCCLUSIVE INFARCT IN ADULT STROKE

By

Neva Leslie Frumkin

A DISSERTATION

Submitted to
Michigan State University
in partial fulfillment of the requirements
for the degree of

DOCTOR OF PHILOSOPHY

Department of Audiology and Speech Sciences

1989

ABSTRACT

MRI AND CT ANALYSIS OF
OCCLUSIVE INFARCT IN ADULT STROKE

By

Neva Leslie Frumkin

Previous studies claim that the brain imaging technique of magnetic resonance imaging (MRI) is the method of choice over computed tomography (CT) for the detection and visualization of stroke. The purpose of this study was to investigate, more specifically, the comparison between lesion size and location of occlusive stroke as demonstrated by CT and MRI.

Data from ten adults, above the age of 20 years, was analyzed in this retrospective study. The subjects were identified to have a single occlusive cerebrovascular accident in either hemisphere on computed tomography, with a confirmed diagnosis of occlusive stroke on a follow-up magnetic resonance imaging study. Three radiologists outlined the boundary of the lesion on all of the CT and MRI images and identified which anatomical structures were involved in the lesion as visualized on each modality.

The analyses led to the conclusions that, in the first few weeks poststroke, the number of reported areas of brain involvement in an occlusive lesion does not differ statistically on the two imaging modalities. The reported location of the lesion also does not differ for lesions which are small, in one lobe of the brain, on or near the cortex, or in a deep structure with circumscribed boundaries. MRI,

however, seemed to allow for a more specific description of the involved areas of the lesion, particularly when located on the border of two different lobes or in deep structures in and around the basal ganglia. It was also found that there was not a statistically significant difference between the size of lesion as visualized on the two modalities. Although not statistically significant, there was a tendency on MRI for more areas to be reported as involved in the lesion and for lesions to be larger.

On the basis of the current investigation, it is likely that future MRI studies correlating lesion size and location with aphasia will generally confirm the findings of previous CT research. Magnetic resonance imaging may allow for a more specific description of the involved areas with lesions located on the border of two different lobes or in deep structures in and around the basal ganglia, along with a more precise determination of lesion extent.

To Miss Lauren A. Frumkin

ACKNOWLEDGMENTS

Interdisciplinary research is one of the most exciting trends in the field of neuroscience. In an interdisciplinary venture, success is intricately dependent on the participation of a variety of people from different backgrounds. The research conducted for this thesis involved the uniting of professionals from the disciplines of speech-language pathology and radiology.

Appreciation is extended to Dr. Gloriajean Wallace, dissertation director, and the other members of my thesis committee who represented the Department of Audiology and Speech Sciences; Dr. Peter LaPine, Dr. Ida Stockman and specifically Dr. Paul Cooke for his additional academic guidance throughout my doctoral program. Special thanks are further extended to committee members Dr. E.J. Potchen and Arlene Sierra from the Department of Radiology, who believed in my work and provided me with four years of unending support, resources, guidance, and challenge.

Beyond my thesis committee members, I am grateful to numerous people within the Department of Radiology who, with their guidance, facilitated the progress of this research. Sincere appreciation is extended to Dr. Jim Moore, Dr. Joe Pernicone, and Dr. Ken Foster who spent many voluntary hours reviewing MRI and CT scans for this project; and Dr. Atis Freimanis who was always available to pull it all together. I must also mention the many other radiologists,

technologists, and clerical staff who were forever willing to assist in any way. These people have become my friends and the information they have shared with me will serve as my professional foundation in the future.

Throughout these past few years it was often difficult to appreciate any life outside of the dissertation. There are many friends who supported me along the way and provided the balance which kept me healthy. A few special people were with me from the beginning every step of the way and were the motivation behind the completion of this degree. I am forever indebted to my friends Diedra and Elaine, my OIALT friend Dr. A. and my husband Yossi. They each own a piece of my Ph.D.

Most importantly, this degree would never have become a reality were it not for my family. My parents, Elaine and Alfred, and my sibs Mitch and Arlene, Lynne, Karen, and Maurice have unquestioningly encouraged me in every project I have ever undertaken. I have survived on their support in the past and will continue to thrive on it in the future. Thank you.

TABLE OF CONTENTS

LIST OF TABLES xii

LIST OF FIGURES xiv

CHAPTER I: INTRODUCTION AND STATEMENT OF THE PROBLEM 1

Introduction 1
Neuroimaging 1
Neuroimaging, Stroke, and Aphasia 3
Statement of the Problem 4
Purpose of the Study 5
Research Questions 6

CHAPTER II: BACKGROUND AND REVIEW OF THE LITERATURE 7

Computed Tomography 7
CT Technique 8
CT Study Parameters 11
Window Settings 11
Contrast Enhancement 12
Slice Thickness 13
CT and Occlusive Infarct in Adult Stroke. . 14
Magnetic Resonance Imaging 16
MRI Technique 17
MRI Study Parameters 19
Pulse Sequence and Pulse Time Intervals 20
Slice Thickness and Interslice Space 21
Field of View and Acquisition Matrix Size 22
Number of Excitations 23
MRI and Occlusive Infarct in Adult Stroke . 23
Summary of the Contrasts Between CT and MRI in their Depiction of Occlusive Stroke 27

Aphasia and Lesion Characteristics 29
Historical Perspective 29
Computed Tomography 32
Recovery from Aphasia 32
Traditional Aphasia Classification 34
Subcortical Lesion Sites and Aphasia 35
Magnetic Resonance Imaging 35

CHAPTER III: METHODS 39

Goal of the Study 39
Subjects and Subject Selection Process 39
Subjects 39
Subject Selection Process 43
Experimental Procedures 43
Computed Tomography 43
Magnetic Resonance Imaging 46
Data Collection 49
Determining Single Lesion on CT . 50
Choosing the Images for Study . . 50
Outlining the Boundary of the Lesion 51
Collecting Anatomical Lesion Location Data 52
Collecting Lesion Size Data . . . 53
Calculating Lesion Area 56
Calculating Final Lesion Volume . 60
Reliability 63
Summary 63

CHAPTER IV: RESULTS 65

Number of Areas of Lesion Involvement as Visualized on Computed Tomography and Magnetic Resonance Imaging. . 66
Research Question One 66
Reliability 71
Size of Lesion as Visualized on Computed Tomography and Magnetic Resonance Imaging 74
Research Question Two 74
Parametric Analysis 74
Reliability of Radiologists' Observations 74
Reliability of Judges' Calculations 77
Confidence of Lesion Size Results 77
Nonparametric Analysis 78
Research Question Three 82

Supplementary Analysis 85
Location of the Target Lesion on CT and MRI 85
Reliability 86
Additional Brain Findings 89
Reliability 92
Diabetes and Hypertension 94
Age 95

CHAPTER V: DISCUSSION AND IMPLICATIONS 96

Localization of Occlusive Stroke Lesions 97
Implications 99
Size of Occlusive Lesion 102
Implications 103
Reliability of Results 105
Limitations of the Study 107
Subjects 107
Computed Tomography Studies 108
Methodology 108

CHAPTER VI: SUMMARY, CONCLUSIONS AND DIRECTIONS FOR FURTHER RESEARCH 110

Summary 110
Conclusions 113
Directions for Further Research 114

APPENDICES

A. Sample of Transparency Used to Outline Lesion 116

B. Anatomical Checklist 117

C. Illustration of Completed Transparency Used in Outlining Lesion 119

D. Illustration of Grid Page with Outlined Lesion 120

E. Measurement Instruction Sheet for Raters 121

F. Illustration of Measurement Grid 122

G. Measurement Instruction Sheet for Raters, Revised 123

H. Illustration of Completed Measurement Grid 124

I. Surface Area of Target Lesion on CT and MRI as Outlined by Three Radiologists and Calculated by Two Judges 125

J. Calculation of Radiologist Outlier 126

K. Surface Area Judgements Used in the Determination of Averaged Surface Area 127

L. Description of Calculation of Lesion Volume on Computed Tomography 128

M. Description of Calculation of Lesion Volume on Magnetic Resonance 129

N. Illustration of Calculation of Lesion Volume on Computed Tomography 131

O. Illustration of Calculation of Lesion Volume on Magnetic Resonance 132

P. Radiologists' Replicated Measurements of Surface Area of Target Lesion on CT and MRI 133

Q. Judges' Replicated Calculations of Surface Area of Target Lesion on CT and MRI 134

R. Distribution of Three Radiologists' Responses With Respect to Anatomy of Lesions Seen on Computed Tomography Scans 135

S. Distribution of Three Radiologists' Responses With Respect to Anatomy of Lesions Seen on Magnetic Resonance Imaging Scans 136

T. Localization of Target Lesions on Computed Tomography and Magnetic Resonance as Reported by Radiologist A . . . 137

U. Localization of Target Lesions on Computed Tomography and Magnetic Resonance as Reported by Radiologist B . . . 138

V. Localization of Target Lesions on Computed Tomography and Magnetic Resonance as Reported by Radiologist C . . . 139

W. Repeated Observations of Lesion Location for Two Subjects on Computed Tomography and Magnetic Resonance by Radiologist A 140

X. Repeated Observations of Lesion Location for Two Subjects on Computed Tomography and Magnetic Resonance by Radiologist B 141

Y. Repeated Observations of Lesion Location for Two Subjects on Computed Tomography and Magnetic Resonance by Radiologist C 142

LIST OF REFERENCES 143

LIST OF TABLES

1. Subject Characteristics 42

2. Parameters of the Contrast Enhanced Computed Tomography (CT) Studies Collected Retrospectively 45

3. Parameters of the Magnetic Resonance Imaging (MRI) Studies Collected Retrospectively 48

4. Averaged Surface Area of Target Lesion on CT and MRI . . 58

5. Volume of Target Lesion on CT and MRI 62

6. Distribution of Radiologists' Responses with Respect to Anatomy of Lesions Seen on Computed Tomography Scans. 69

7. Distribution of Radiologists' Responses with Respect to Anatomy of Lesions Seen on Magnetic Resonance Scans . 70

8. Interjudge Reliability for Number of Affected Brain Areas Reported by Three Radiologists for CT and MRI 71

9. Intrajudge Reliability for Number of Affected Brain Areas for Three Radiologists for CT and MRI 73

10. Inter- and Intrajudge Reliability for Size of Lesion on CT and MRI as Determined by Three Radiologists . . . 76

11. Correlational Coefficient (rho) Between Volume of Lesion on Computed Tomography and Magnetic Resonance Imaging. . 79

12. Summary Statistics for Volume of Target Lesion on CT and MRI 84

13 Location of Target Lesion as Visualized on Computed Tomography 87

14. Location of Target Lesion as Visualized on Magnetic Resonance Imaging 88

15. Additional Brain Findings Visualized on Magnetic Resonance Imaging Not Visualized on Computed Tomography 91

16. Repeated Observations of Additional Brain Findings as Visualized on Magnetic Resonance Imaging for Two of the Ten Subjects 93

LIST OF FIGURES

1. Scattergram Depicting the Relationship Between Volume of Lesion on CT and MRI for 10 Subjects. 81

CHAPTER I

Introduction and Statement of the Problem

Introduction

Neuroimaging

Before the late 1960s, the technique available for imaging the anatomy of the body and head was traditional shadow radiography also known as plain x-ray (Oldendorf, 1985). A radiograph, or x-ray, depicted the amount of x-radiation that passed through the body (Trapnell, 1967). The amount of obstructed, or attenuated, x-ray was determined by the density of body structures through which the radiation passed and these differences in densities allowed for visual differentiation of anatomical entities.

For disorders of the central nervous system, the value of plain radiographs as a diagnostic tool has always been especially limited (Straub, 1984; Trapnell, 1967). The resolution of traditional radiographs of the brain are limited to depicting differences in attenuation values which are more than two percent (Katz, 1984; Martin & Brust, 1985). For example, the gray and white matter of the brain cannot be distinguished due to their similar absorption of x-rays. Cerebrospinal fluid and soft tissues, which constitute the bulk of the central nervous system, have similar radiographic densities and differentiation between these anatomical entities is also limited. Plain radiographs of the head showed only abnormally dense or

abnormally thin areas within soft tissue, and their effects on the surrounding skull (Trapnell). Finer distinctions in densities were not visible on the traditional plain film radiographs. The problem of superimposition of structures was another major shortcoming of the technique (Katz, 1984).

Since the late 1960s, two imaging techniques have become clinically available which have revolutionized the field of neuroradiology. The brain imaging techniques of computed tomography (CT) and magnetic resonance imaging (MRI) have substantially improved the selection of tools available for the diagnostic and clinical management of central nervous system disease.

Computed tomography is based on the use of radiation and has been available for clinical use since the late 1960's. CT detects radiation that has passed through the body at multiple angles and then, with the aid of a computer, reconstructs a cross section of absorbtion values for the section of the body or head being studied (Villafana, 1983). CT allows visualization of the anatomy and pathology of the central nervous system based on the structural densities of the area of study.

Magnetic resonance imaging has been available for clinical use since the late 1970's and is based on the use of magnetic forces both within and outside the body. MR images depict densities of spinning nuclei within structures being studied, in addition to other magnetic properties of the nuclei. Each tissue in the body consists of a different composition of nuclei and these variations allow MRI to be sensitive to differences between body tissues. MR images can be directly obtained in unlimited planes of angle and, since there are no

moving nuclei in bone, visualization of anatomical structures is not obscured by bone artifacts on the images (Bydder et al., 1982).

Strengths and weaknesses of the CT and MR imaging techniques have a bearing on which is the more valid procedure for visualizing specific disease entities. Numerous studies have been done which compare the techniques of CT and MRI in their depiction of CNS disease, specifically stroke (Brown, Hesselink, & Rothrock, 1988; Bydder et al., 1982; DeWitt et al., 1984; Kinkel, Kinkel, & Jacobs, 1986; Kistler, Buonanno, Roh, & Davis, 1986). Typically, these studies have investigated the two imaging techniques in regard to their sensitivity and specificity to disease (Brant-Zawadzki et al., 1983; Haughton et al., 1986). Sensitivity is defined as "the proportion of diseased patients who are reported positive" and specificity as "the proportion of patients free of the disease who are reported negative" (Freedman, 1987). There is a paucity of detailed, quantitative comparisons between the two imaging techniques in regard to their ability to localize or determine the extent of lesions.

Neuroimaging, Stroke, and Aphasia

Computed tomography is currently the most commonly used radiological study done for the evaluation of stroke (Wang, Lin, & Rumbaugh, 1988). Information gained from computerized tomography is routinely used in patient medical management. Furthermore, information from computed tomography has also been used in the formulation of theories which are used to guide the clinical management of speech and language consequences of stroke, namely aphasia.

CT research has had a significant impact on many aspects of the study of brain-behavior relationships in aphasia. The most frequent topic in aphasia to be studied with the use of computed tomography brain imaging has been recovery (Yarnell, Monroe, & Sobel, 1976; Kertesz, Harlock, & Coates, 1979; Naeser, Helm-Estabrooks, Haas, Auerbach, & Srinivasan, 1987). The next most frequent area of CT aphasia research has been localization of lesion and classification of aphasia types (Naeser & Hayward, 1978; Mazzocchi & Vignolo, 1979). Recently, attention has begun to focus on noncortical lesions producing aphasia (Damasio, Damasio, Rizzo, Varney, & Gersh, 1982; Naeser et al., 1982). A thorough review of these studies and others can be found in Chapter II, Background and Review of the Literature.

Statement of the Problem

Theories regarding brain-behavior relationships should be based on the most accurate and advanced information available regarding the brain and its relationship to language. The present revolution in neurodiagnostic procedures is significantly increasing the information available in the understanding of this relationship. With the emerging use of magnetic resonance imaging in the evaluation of stroke, more specific information is becoming available for the study of brain-behavior relationships in aphasia. Currently, MRI information is beginning to accumulate along with the more traditional CT information. Less attention, however, has been directed to quantitative comparisons between the two techniques.

There has always been a need to quantitatively evaluate and

compare alternative diagnostic approaches (Freedman, 1987; Potchen, 1975). Since the introduction of magnetic resonance imaging, most clinical studies comparing CT and MRI have reported that MRI is the method of choice for detecting infarction (Brant-Zawadzki, et al., 1985; Pykett, Buonanno, Brady, & Kistler, 1983; Sipponen, 1984; Sipponen et al., 1983). Although studies have been done regarding sensitivity to disease detection, quantitative comparisons between the two techniques for determination of lesion location and extent have not been completed.

In the past, information regarding lesion location and extent, obtained from computerized tomography, has been used in the formulation of theories regarding aphasia classification and prognostic indications for aphasia recovery. With the recent advent of magnetic resonance imaging as a clinical tool, a quantitative comparison between stroke information available from CT and MRI is compelling. A difference in the amount and type of information obtained from CT and MRI might have implications for the accuracy of currently held beliefs in the field of aphasiology.

Purpose of the Study

The purpose of this retrospective study was to determine if lesion site and extent information gained by magnetic resonance imaging was comparable to lesion site and extent information gained by computed tomography, from images in the axial plane. The study attempted to quantify the differences between the methods of CT and MRI in defining size and location of lesion in occlusive stroke.

Research Questions

1. Is there a significant difference in the number of primary area(s) of lesion involvement when comparisons are made for MRI and CT axial image measurements?

2. Is there a significant correlation between size of primary lesion for MRI and CT axial measurements?

3. Is there a significant difference between the size of lesion on CT and MRI?

CHAPTER II

Background and Review of the Literature

The first section of this chapter presents background information and a review of the literature in regard to the brain imaging technique of computed tomography. The discussion of the technique of CT is followed by a review of the literature pertaining to the use of computed tomography with occlusive infarct in adult stroke. The second section of this chapter details the same information listed above, but for the brain imaging technique of magnetic resonance imaging. A summary of the contrasts between the techniques of CT and MRI in the depiction of occlusive stroke is followed by a review of CT and MRI aphasia research.

Computed Tomography

The mathematical basis for computed tomography, reconstruction of an object from an infinite set of measurements, was established by an Austrian mathematician in 1917 (Katz, 1984). For approximately the next 50 years, scientists attempted to develop and refine a medical application for the mathematical theory of image reconstruction. It was not until the late 1960's when the first practical model of a computerized reconstructive scanner was developed by Godfrey Hounsfield and his colleagues in Great Britian (Katz). Hounsfield's interest in reconstruction techniques using the computer lead to the

development of the first clinically useful computed tomography scanner (Seeram, 1982). This advancement in imaging was so significant that it won its inventors the Nobel Prize for Physiology and Medicine in 1979 (Martin & Brust, 1985). Approximately five years after its development, in 1973, the first CT brain scanners were installed at the Mayo Clinic and the Massachusetts General Hospital in the United States (Seeram).

CT Technique

Computed tomography is a technique in which a computer reconstructs the internal structure of a selected body section (Weisberg, Nice, & Katz, 1984.) The method used in computed tomography is to detect radiation that has passed through the body at multiple angles and then to mathematically reconstruct a cross section of absorption values by the use of a computer algorithm (Villafana, 1983). Many narrow beams of x-rays are directed into the selected body section from multiple directions. The absorption information generated in CT is collected with the aid of a computer as numerical values which are eventually converted into a pictoral display (Oldendorf, 1985). This computerized display is quite different than the direct x-ray picture taken of a body section in plain radiograph films.

Attenuation, in which the x-rays are reduced in intensity on passing through objects, (Carroll, 1985) depends on structural densities. Although the densities of gray and white matter, blood, and cerebrospinal fluid differ very little, computer analyzed x-ray attenuation values as employed in CT allow differentiation (Martin &

Brust, 1985). The distribution of CT attenuation values has been established on a relative scale with the attenuation of water as a reference (De Groot, 1984). This scale is measured in Hounsfield units (HU), named for its inventor. On the two extremes of the scale, bone and air have values of +1000 and -1000 Hounsfield units (HU), respectively. Once these attenuation values are obtained, the numerical image can be converted to a gray scale image in which bone is represented as white, air is represented as black, and all other values represent varying shades of gray (Seeram, 1982). White indicates a structure which is high in density where much of the CT x-ray beam is absorbed. Black indicates a low density structure where little of the x-ray beam is absorbed. One Hounsfield unit represents a 0.1 percent change in attenuation relative to water (Carroll).

Pencil thin x-ray beams are used in CT scanning. These beams are obtained by a collimation process in which the divergent portion of the x-ray beam is eliminated. The resulting collimated beams have a finite width which allows attenuation coefficients to be reconstructed for specific volume elements, or sections, of the object being scanned (Seeram, 1982). These volume elements are called voxels. A typical volume element in CT measures 10 mm. in depth, 1.0 mm in width, and 1.0 mm in length. The voxel is displayed as little squares or picture elements called pixels on the CT image.

Since computed tomography is based on the use of x-radiation, the patient is exposed to radiation during the study. There are a number of variables in the CT scan procedure that influence the dose of radiation to which the patient is exposed (Seeram, 1982). In general, the radiation dose is related to the basic imaging parameters of the

CT unit. These include slice thickness of the images, collimation levels of the x-ray beams, and x-ray detector efficiency. For standard operation, most CT units have a maximum entrance dose of about 2 to 5 rads, or units of radiation dose, per area of study (Seeram). Radiation dose does not sum across areas of the body, however it does significantly increase if the same area is repeatedly studied (Villafana, 1983).

The standard CT scan image is of the transverse axial plane. Although there is not universal agreement on a standard plane of section, the planes most commonly used are those angled 25 or 35 degrees to an anatomical baseline (Hanaway, Scott, & Strother, 1980). This zero point, called Reid's baseline, runs from the superior orbital rim to the top of the external auditory meatus. The patient is aligned at the desired angulation relative to Reid's baseline. The desired angulation is achieved by tilting the head rest. In the past, sagittal and coronal CT images could be acquired by removing and repositioning the patient (Villafana, 1983). More recently, computer programs have been developed to mathematically reconstruct these other plane slices using the information obtained from the standard transverse scans (Villafana). The use of multiplanar reconstruction may produce artifacts or inaccuracies on the resulting images due to mathematical problems with data reconstruction (Katz, 1984; Seeram, 1982). Each supplementary study also subjects the patient to additional doses of radiation (Seeram).

There have been numerous generations, or models, of CT scanners developed (Villafana, 1983). Each generation of machine improved upon the method of computerized data collection (Katz, 1984). The number,

arrangement, and motion of the x-ray beams and detectors were altered and refined with each update (Katz). In the fourth generation scanners, which are the machines currently in use, the x-ray tube moves around the patient and a full circle of detectors remains stationary. Each detector views a rotating x-ray source which allows for a higher spatial resolution. Spatial resolution refers to the ability to discriminate objects of limiting size or proximity (Seeram, 1982). Tomography, as in computed tomography, refers to the use of moving x-ray tubes, body parts, or x-ray image receptors to desuperimpose obstructing anatomy from the anatomy of interest (Carroll, 1985).

CT Study Parameters

Window Settings. The range of x-ray absorption values used for a CT scan may be manipulated according to what is being examined. When collecting head scans, control settings such as window width and window center are at the discretion of the controller (Koehler, Anderson, & Baxter, 1979). Window width refers to the range of x-ray absorption values, or the sensitivity setting, selected for a particular study (de Groot, 1984; Koehler, Anderson, & Baxter). Window center refers to the center of that segment of the total scale of absorption values (Koehler, Anderson, & Baxter). The settings chosen for a particular study determine which portion of the total available range of CT attenuation values are displayed in the resulting image. Optimal settings for best visualization of pathology varies with different scanner models (Weisberg, Nice, & Katz, 1984). Generally, since tissue densities in the brain fall within a narrow

range, control settings for a brain study are chosen in a standard fashion (Koehler, Anderson, & Baxter). Routine scans of the brain are usually done at window width settings of 80 to 150 Hounsfield Units (de Groot). If a window width of +80 is chosen, all attenuation values higher than +80 will appear white, those less than 0 will appear black, and all values between 0 and +80 will appear as shades of gray (Katz, 1984).

Contrast Enhancement. Computed tomography scans can be obtained with or without contrast enhancement. Contrast enhancement refers to the method of improving visualization of certain structures and tissues by the use of iodinated contrast material (Seeram, 1982). In a contrast enhanced study, radiopaque contrast material is injected intravenously prior to collecting a CT scan (Martin & Brust, 1985). The injection of contrast allows enhancement of regions of the brain which have either increased vasculature or an impaired blood-brain barrier. With an intact blood-brain barrier, the brain and its cerebrospinal fluid is naturally protected against harmful elements which may be in the blood of the body (Rowland, 1985). The barrier is a complex combination of morphological and functional characteristics of brain capillaries (Rowland). In many diseases, the blood-brain barrier does not function effectively and elements which are typically excluded from entering the brain can pass through. If there is a breakdown in the blood-brain barrier, radiopaque contrast material injected in a CT study can also pass into the vascular spaces of the brain (Goldberg, 1983).

Ischemic stroke results in a positive CT scan in 66 to 98 percent of cases (Goldberg, 1983). Additional information may be obtained if

CT scans are performed with the injection of intravenous contrast material. Injection of a contrast material increases the density of cerebral infarcts which allows for improved visualization of lesion extent. Contrast-enhanced CT scans detect up to 13 percent of infarcts which were invisible on noncontrast CT scans (Goldberg). Contrast enhancement is most effective between approximately the fifth day poststroke and week three or four (Yock, 1985; Zulch, 1985). By the third week, up to 95 percent of infarcts will enhance after the injection of contrast material (Zulch). Time of peak enhancement is dependent on changes in tissue density and the development of edema within the brain after stroke (Zulch). It has become almost routine to perform enhanced scans in many medical centers (Weisberg, Nice, & Katz, 1984).

Slice Thickness. The thickness of a slice of anatomical information chosen for a CT study is variable. The thicker the slice, the more information is mathematically averaged together within the section. Extremely thin slices (below 1 mm), however, are generally not possible due to technical restrictions such as the distance of the x-ray beams, nor advisable due to the dose of radiation inflicted on the patient (Alexander, Kalender, & Linke, 1986). Furthermore, if thinner slices are used, more slices need to be studied which increases the amount of time for an examination (Katz, 1984). Slice thickness in CT studies can vary between 1 to 10 mm, but for standard studies is generally set around 10 mm. CT slices are usually contiguous, or aligned adjacent to each other, with no space between slices.

CT and Occlusive Infarct in Adult Stroke

The introduction of computed tomography as a brain imaging technique greatly enhanced the capabilities for stroke diagnosis and management. Information gained by CT added significantly to the knowledge available regarding the effect of stroke on the brain.

A CT scan may appear almost or completely normal prior to the eighth hour after stroke (Wang, Lin, & Rumbaugh, 1988). Then, depending on the size and location of the infarct, the first evidence of ischemia may appear. Between the eighth and 24th hour poststroke, a noncontrast CT may demonstrate a slight hypodense (dark) area with poor margins and a spotty appearance (Goldberg, 1983). Edema may cause effacement, or the smoothing over appearance of cortical sulcal spaces (Weisberg, Nice, & Katz, 1984). During this first 24 hours there is little or no swelling or mass effect evident (Goldberg, 1983). Small lesions, without significant edema, may not become apparent until later in the chronic stage when a cystic lesion forms (Goldberg). Cerebellar and brainstem lesions have a low incidence of detection because they are small and hidden by bone artifacts.

After a few days, the hypodense area representing infarction becomes more distinct. It may take on a triangular, rectangular, trapezoid, round or oval shape depending on the occluded artery and the vascular territory involved (Bories, Derhy, & Chiras, 1985). The most common pattern is a wedge-shaped hypodense lesion indicating an infarct in the territory of the middle cerebral artery (Weisberg, Nice, & Katz, 1984; Zulch, 1985).

From the third to the fifth day, the low density area becomes more homogeneous with sharper edges and the area of hypodensity

increases (Goldberg, 1983). It is during this time that edema and tissue death are increasing and reaching their maximum. Swelling and mass effect depend on the size of the infarct. Some degree of mass effect is reported in 21 to 70 percent of infarcts and is most evident between the third and fifth days (Goldberg). Swelling, causing mass effect, and edema begin to decrease after the first week and by the 12th to 21st day are usually completely resolved (Goldberg; Weisberg, Nice, & Katz, 1984).

During the second and third weeks, curvilinear bands which are either hyperdense (bright) or isodense (same intensity as surrounding brain) often develop at the margins of or within the infarcted area (Goldberg, 1983). These bands are a result of new capillary ingrowth, improved circulation, or hemorrhage within the infarct. These bands cause the boundaries of the lesion to become less sharp than on earlier scans. Due to an increase in density of the lesion on CT during this time, the lesion may become isodense (the same intensity) as the surrounding brain making it hard to visualize. This phenomenon, which may occur during the second or third weeks poststroke, is called the 'fogging effect' (Bories, Derhy, & Chiras, 1985; Weisberg, Nice, & Katz, 1984)

Starting at approximately one month post stroke and continuing for two to three months, the resorption phase begins (Weisberg, Nice, & Katz, 1984). The outline of the infarct becomes sharp and the hypodense area begins to appear smaller due to absorption of the necrotic tissue and resolution of edema (Weisberg, Nice, & Katz). Depending on the size and location of the infarct, atrophy from the necrotic brain tissue may cause the lateral ventricles to dilate and

shift toward the infarcted area, and there may be a shift of the brain midline to the side of the infarct. Atrophic change, demonstrated by a shrinking of the brain and widening of the sulci, may also be seen in the overlying cortex to the infarct. Beginning in the fifth week poststroke, many necrotic infarcts become fluid-filled cysts which have a low attenuation value on CT similar to cerebrospinal fluid (Wang, Lin, & Rumbaugh, 1988). By the end of the third month, chronic brain changes are usually complete and there is usually no further change in size or appearance of infarcts (Goldberg, 1983; Weisberg, Nice, & Katz).

Magnetic Resonance Imaging

The use of magnetic resonance imaging in the medical field may be relatively new, however, scientists have employed the technique of nuclear magnetic resonance spectroscopy in the laboratory for nearly 40 years. The technique has developed into one of the most important methods used in chemistry for measuring the atomic constituents of chemical samples (Gademann, 1984; Martin & Brust, 1985). The present surge of interest in medical applications for magnetic resonance imaging stems from two studies done in the 1970's. Using rats, Raymond Damadian (1971) found that magnetic resonance imaging could be used for discriminating between malignant tumors and normal tissue. P.C Lauterbur (1973) found that an image of an object could be generated by a graphical representation of the spatial distribution of its properties. These studies, in conjunction with the successful impact of CT on the field of medical imaging, motivated research in

the area of magnetic imaging (Kean & Smith, 1986).

The first experimental MRI scan of a human being was performed in 1977 (Bydder & Steiner, 1982). In the early 1980's, after years of intensive developmental work on the MR imaging systems, the focus of attention shifted from machine development to clinical results (Gademann, 1984). In March 1984, the FDA permitted two American companies to begin commercial sales of the devices to hospitals and physicians (Bydder & Steiner).

MRI Technique

The technique of magnetic resonance imaging uses the inherent property of spinning atomic nuclei in the body (Gademann, 1984). A large superconducting magnet is used to impose a magnetic field on the object of study (Gademann). Once the nuclei in the section of study are aligned by the large magnetic field, additional smaller magnets apply radio frequency (RF) energy to the spinning elements and tilt them at various angles. The nuclei now spin on a tilted axis to the main magnetic field. When the RF energy is switched off, MR images are produced during relaxation of the excited nuclei (Jones et al., 1985). The relaxing nuclei emit a signal which is computer processed. These digital data are transformed into pictorial information demonstrating the brain's gray and white matter as well as cerebral spinal fluid. Images reflect the density of the spinning nuclei in the area of study and the rate at which various substances in the region relax. These measurements vary according to the composition of the anatomic regions under study.

Magnetic resonance systems vary in the strength of their magnetic field. The strength of the magnet used has a direct influence on the resolution of images. Tesla refers to the unit of magnetic field density used in MR imaging (Elster, 1986). One Tesla (T) is equal to 10,000 gauss or 10,000 times the approximate strength of the earth's magnetic field on its surface (Elster). MR systems using magnetic fields greater than 0.5 Tesla are considered high field and those with magnetic fields less than 0.5 Tesla are considered low field systems.

MR imaging is a noninvasive procedure and does not employ the use of ionizing radiation (Jones et al., 1985). However, the entire process is based on the use of powerful magnets. Implanted ferromagnetic objects, (which contain iron) such as surgical clips, heart valves, orthopedic implants, or cochlear implants are a contraindication for MR imaging. Most surgical clips, virtually all modern types of heart valves, and most orthopedic implants are only weakly if at all ferromagnetic and pose no problems during MR examination (Pavlicek, 1988). Cardiac pacemakers have specifically been identified as a hazard for MR examination (Laakman et al., 1985; Pavlicek et al., 1983). The major concern with a pacemaker is possible damage to its electronic components as a result of the strong MR magnetization (Pavlicek).

MR images are not obscured by bone. There are no spinning nuclei in bone which would be affected by the magnetic forces applied to the body, thus no signal is emitted (Gademann, 1984). Due to the fact that bone does not emit a signal and therefore does not obscure visualization of other anatomic areas of the brain, infarctions which are located on or near the cortex, posterior base of the brain or the

brainstem are well visualized on MRI (Kinkel, Kinkel, & Jacobs, 1986).

Magnetic resonance images reflect the density of spinning nuclei, and other magnetic properties of the tissues in the body. Since a variety of information is collected and analyzed in an MR scan, there can be a higher degree of differentiation between body tissues than has been possible with other techniques based solely on structural densities (Bradley, 1986). One of the greatest advantages of MRI is its unprecedented ability to display differences in gray and white matter of the brain (Bydder et al., 1982). This sensitivity to gray/white distinctions allows superb visualization of deep basal ganglia structures and white matter fibers of the brain.

On all MR scanners, an option exists for obtaining images in orthogonal, right angle, planes in the human head (Gademann, 1984). Axial, sagittal, and coronal images are directly obtainable from the digital data collected during the MR study without the need to reposition the patient or perform computer reconstructions (Elster, 1986). Unlimited, or oblique planes of study are furthermore available, depending on the computer software capabilities of the respective system (Elster).

MRI Study Parameters

The appearance of structures in an MR image is determined by specific intrinsic characteristics of the tissues being studied and operator selected extrinsic parameters (Wehrli & Rield-Quick, 1988). There are three main intrinsic parameters which are specific to each tissue. After the magnetic forces are applied to the body section of study, these three parameters determine to a large extent, how the

resulting images will appear. The three tissue characteristics are: (1) the density of the spinning nuclei in the area of study (Spin Density), (2) the time it takes for the nuclei to relax back from their tilts to realign with the main magnetic field (T1), and (3) the time it takes for the nuclei to dephase or lose their coherence with each other (T2). Each tissue in the body is made up of a different composition of nuclei. Variations in these three intrinsic factors are responsible for the extreme sensitivity MRI has to differentiate between body tissues.

Pulse Sequence and Pulse Time Intervals. In addition to intrinsic characterisics of body tissues, extrinsic operator-controlled parameters can also be adjusted in order to gain different types of information. The appearance of the images can be adjusted or "weighted" depending on the pattern and timing of the magnetic pulses applied to the area of study (Crooks et al., 1982). The sequencing of magnetic pulses can be adjusted to emphasize different degrees of spin density, T1 or T2 in the resulting image. Specific adjustments can enhance various characteristics of tissues, for example, T1 weighted images provide excellent anatomical differentiation while T2 weighted images are more sensitive to variations in fluids and pathology.

The magnetic forces in MR can be applied in specific sequences of pulses to enhance certain characteristics of an image (Gademann, 1984). There are virtually unlimited combinations of pulses which may be applied to a tissue to generate an MR signal (Elster, 1986). The selection of a pulse sequence is at the core of magnetic resonance imaging and ultimately affects the detection and characterization of

lesions (Elster; Posin et al., 1985). All pulse sequences use a combination of 90 and 180 degree pulses of radiofrequency energy. The order of these pulses and the time intervals between the pulses are the parameters which make the various pulse sequences unique (Elster). The two parameters, which are common to all pulse sequences, are referred to as: Repetition Time (TR), the time interval between pulses and Echo Time (TE), the time which elapses between the excitation pulse and the detection of the resulting, emitted signal (Gademann). The most typical options for these two time intervals are TR = 250 - 4000 msec and TE = 20 - 120 msec (Elster).

The Spin-echo pulse sequence is the most common magnet pulse sequence used in medical imaging applications (Elster, 1986; Wehrli & Field-Quick, 1988). In this sequence, after the nuclei of study are aligned with the large static magnetic field, they are pulsed by the radiofrequency (RF) energy at a 90 degree pulse. This is followed by a time interval (TR) and then a 180 degree pulse. This is followed again by a time interval and then the signal is measured (TE). The spin-echo pulse sequence results in the enhancement of the T2 relaxation time, or the time it takes the nuclei to loose their coherence with each other (Gademann, 1984). Spin-echo images highlight pathological change such as lesions and edema.

Slice Thickness and Interslice Space. Slice thicknesses from generally 2 mm to 10 mm are available on commercial MR scanners (Elster, 1986). As with CT, there is a trade-off between thickness of slice, signal intensity, and scanning time. Thinner slices, although they may demonstrate finer anatomical detail, require longer times to scan (Elster). The signal-to-noise ratio, or the proportion of noise

to the signal, also gets less desirable as the slices get thinner. The thicker the slice, however, the more information is averaged into an image (Wehrli & Field-Quick, 1988). Typical options for slice thickness are 3, 5, 7, and 10 mm (Elster). Unlike standard CT, MRI image slices are not contiguous. Since there is some partial excitation of neighboring tissues outside of the area of study in MR, it was determined that inserting gaps between the slices was an effective correction for the overflow of magnetic force. Typically, an interslice space is 25 to 50 percent of the actual slice thickness ie. 2.5 mm for a study with 5 mm slice thickness (Wehrli & Field-Quick).

Field of View and Acquisition Matrix Size. Field of view (FOV) and acquisition matrix together determine the size of pixels and therefore spatial resolution in an MR image (Wehrli & Field-Quick, 1988). Each square of pictorial information on the image is called a pixel (picture element) (General Electric, 1984). Most MR scanners offer matrices from 128 X 128 to 256 X 256 (Elster, 1986). This two dimentional matrix size indicates the number of pixels in a particular field of view. If a matrix of 256 X 256 is employed, there will be 256 X 256 pixels of pictorial information contained within a section of view. If the field of view is 24 centimeters, then the 256 X 256 pixels of information is contained within 24 centimeters. As with the other operator controlled parameters, there is a trade-off with field of view and matrix size (Elster). A 256 X 256 matrix will show finer detail than a 128 X 128 matrix, however scanning time increases and the signal-to-noise ratio becomes less desirable.

Number of Excitations. One way to counterbalance the use of a finer matrix size and maintain the same signal-to-noise ratio, is to increase the number of times the tissues in a particular section of the body is sampled (Wehrli & Field-Quick, 1988). Number of excitations (NEX) refers to the number of times the same area of tissues is excited. By repeating the number of times an area of tissue is excited, the signal-to-noise ratio improves and therefore the quality of the image improves (Elster, 1988; Wehrli & Field-Quick). At the same time however, each additional NEX increases the time it takes to complete a scan. Two or four repeated excitations is typical of most MR studies (Elster).

MRI and Occlusive Infarct in Adult Stroke

The first descriptions of cerebral abnormalities visualized on magnetic resonance imaging were published in the early 1980's (Bydder, 1984). Many of these reports suggested that MRI is more sensitive in the detection of cerebral pathology than CT (Brant-Zawadzki, et al., 1983; Brant-Zawadzki, et al., 1985; Bydder & Steiner, 1982). These early publications included reports that infarction was well demonstrated on MR.

The strongest determinant of signal change on an MR image during the period of ischemia and subsequent infarction is the acute increase in the water content of tissue (Brant-Zawadzki, 1988). Water is chiefly composed of hydrogen elements (each water molecule has two hydrogen nuclei), and hydrogen is the nucleus studied in magnetic resonance (Bradley, 1987). Water is, in fact, the greatest contributor to the MR signal detected from a voxel of tissue

(Bradley). MRI is therefore a unique tool for the investigation of ischemia and infarction because of its sensitivity to changes in water and therefore its sensitivity to stroke disease (Unger, Littlefield, & Gado, 1988).

The concentration of brain water starts to change in the first hours after an ischemic event (Brant-Zawadzki, 1988). There is an accumulation of water within the cells of the affected area, which is referred to as cytotoxic edema (Brant-Zawadzki & Kucharczyk, 1987). Cytotoxic edema is a result of ischemia and is found in association with acute infarcts (Bradley, 1987). Within the first 30 minutes of ischemia, there is a 3 to 5 percent increase in the water content in the area (Brant-Zawadzki & Kucharczyk). These changes in water content allow MRI to detect pathology within the first hour or two following vascular occlusion (Brant-Zawadzki).

By the sixth hour, the blood-brain barrier typically begins to break down which allows additional leakage of water and protein from the vascular spaces (Brant-Zawadzki & Kucharczyk, 1987). This secondary process of edema is called vasogenic edema and continues to occur for the first few days poststroke producing mass effect in and around the area of the infarct.

During the initial stage of ischemia, both the T1 (the time it takes for the nuclei to relax back from their tilts to realign with the main magnetic field) and the T2 (the time it takes for the nuclei to dephase or lose their coherence with each other) relaxation rates are prolonged on MRI indicating the water accumulation (Kinkel, Kinkel, & Jacobs, 1986). Prolonged relaxation time on a T1 weighted image will cause the area of ischemia to look like a low intensity

(dark) zone. On T2 weighted images the area of ischemia will present as high intensity (bright). T2 images tend to be more sensitive to changes (cytotoxic edema) at the very earliest hours poststroke (Moseley, 1988; Sipponen et al., 1983). The ischemic evolution, including mass effects, progresses for the first three to seven days and typically stabilizes in the second week (Kinkel, Kinkel, & Jacobs; Sipponen et al.).

A high percentage of ischemic infarcts may be complicated by hemorrhage. Up to 42 percent of patients who initially present with ischemic infarcion develop secondary hemorrhage (Brant-Zawadzki, 1988). Within the evolution of infarction from mass effect to the resolution stage, usually in the second week following infarction, a small amount of leaking blood may escape from the cite of damage. These hemorrhages are generally silent clinically. Acute hemorrhage within an area of infarction will be demonstrated by an excessive shortening of T2 relaxation time, or a low signal (dark) area on T2 weighted images. Differentiation between edema and acute hemorrhage may only be visible on high field MR systems.

Whether combined with hemorrhage or not, after approximately the second week, infarcts evolve in a typical pattern (Brant-Zawadzki, 1988). By the third week and into the chronic stage in the evolution of the infarct, mass effect and edema begin to resolve and subsequent atrophy develops (Kinkel, Kinkel, & Jacobs, 1986; Brant-Zawadzki & Kucharczyk, 1987). Cells may die in the necrotic areas of the brain and tissues may become soft due to greater water content. Encephalomalacia or 'soft brain' is demonstrated as high signal intensity (bright) on T2 weighted images. With lacunar infarcts,

which are small infarcts that lie in the deeper noncortical parts of the brain (Fisher, 1982; Mohr, 1982), the brain usually shrinks and a cyst with cerebrospinal fluid fills in the area. T2 weighted images demonstrate decreased signal intensity from these cyst areas, similar to the signal intensity of cerebrospinal fluid in other parts of the brain (Kinkel, Kinkel, & Jacobs).

Small areas of 'High Signal Intensity' (HSI) are a common finding on MRI in the deep white and deep gray basal ganglia areas of patients over the age of 65 (Brant-Zawadzki, 1988). The bright areas are especially common in elderly persons with a history of cerebral vascular disease risk factors such as hypertension and/or diabetes (Awad, Spetzler, Hodak, Awad, & Carey, 1986; Fezekas et al., 1988; Kertesz et al., 1988; Sarpel, Chaudry, & Hindo, 1987). White matter signal alterations, which represent changes in the water content of the brain, are thought to represent either areas of demylination or small subclinical strokes (Agnoli & Feliciani, 1987; Sarpel, Chaudry, & Hindo). Even in patients without a history of risk factors, 20 to 30 percent of the elderly population display multiple areas of high signal intensity on MR images (Brant-Zawadzki, 1988).

A possible cause suggested for the small subclinical strokes and/or demyelination found on MRI in the elderly is decreased blood flow, or vascular insufficiency, which occurs in the brain with aging (Braffman et al., 1988). This is especially true in the deep hemispheric region of the brain where brain perfusion diminishes with aging (Brant-Zawadzki & Kucharczyk, 1987). CT has been found to be much less successful in demonstrating the areas of high signal intensity found in the brain on MRI (Lechner et al., 1988).

Summary of the Contrasts Between CT and MRI in their Depiction of Occlusive Stroke

Computed tomography is a technique in which a computer reconstructs the internal structure of a selected body section. The method used in computed tomography is to detect radiation that has passed through the body and then to mathematically reconstruct a cross section of the area based on the absorption values of the radiation. Magnetic resonance imaging is a technique which uses the inherent property of spinning atomic nuclei in the body to obtain information. MR images are produced during relaxation of nuclei which had been excited by various magnetic forces. The relaxing nuclei emit a signal which is computer processed.

There are three major differences in the techniques of CT and MRI which apply to studies, including those of stroke. Both CT and MRI parameters can be set for image slice thickness between 1 and 10 mm, however CT images are typically contiguous whereas MR images are not but instead have an interslice space between images. Secondly, the standard CT scan image is in the transverse axial plane. Other planes of study require either repositioning of the patient or mathmetical reconstruction of the information obtained in the standard scan. In contrast, on all MRI scanners, the option exists for obtaining images in orthogonal axial, sagittal, and coronal planes. Some MRI machines also have the capability to directly collect unlimited or oblique planes. Lastly, since computed tomography is based on the use of x-radiation, the patient is exposed to radiation during the CT study. MRI is a noninvasive procedure which does not employ ionizing

radiation. Due to the use of powerful magnets however, patients with implanted metal objects which are made of ferromagnetic materials are not candidates for MRI.

There are additional differences between the brain imaging techniques of computed tomography and magnetic resonance which have specific relevance to the study of stroke. To begin, the only characteristic which is reflected in a CT image is structural densities. Structures with densities which differ very little cannot be differentiated by the technique. In contrast, MRI images reflect the density of spinning nuclei in the area of study along with relaxation characteristics of the various tissues after the application of magnetic forces. This allows MRI to differentiate between tissues based on their composition. Due to this sensitivity, MRI can detect changes in water content indicative of ischemia within the first few hours after stroke whereas a CT scan may appear almost or completely normal many hours poststroke.

Window settings, or the range of x-ray absorption values, used for a CT scan may be manipulated according to what is being examined. This allows the sensitivity setting to be selected from a range of available attenuation values. In addition, the injection of iodinated contrast material is employed in CT studies to improve the visualization of certain structures and tissues. The appearance of images on MR can be adjusted or 'weighted' by manipulating the pattern and timing of the magnetic pulses applied to the area of study. Specific adjustments in the operator controlled parameters can enhance various characteristics of the tissues depending on the nature of the study. The sensitivity MRI has to the composition of tissues, and the

ability to adjust the weighting of the image, allows superior differentiation of gray and white matter both cortically and deep within the brain.

Bone does not emit a signal on MRI therefore structures are not obscured by bone artifacts. Infarcts which are located on or near the cortex, in the posterior base of the brain or in the brainstem are well visualized on MRI. Cerebellar and brainstem lesions have a low incidence of detection on CT because they are small and hidden by bone artifacts.

Due to its superior spatial resolution, MRI is sensitive to small, deep, areas of subclinical strokes and/or demylination. On CT, small lesions without significant edema may not become apparent until later in the chronic stage when a cystic lesion forms.

Aphasia and Lesion Characteristics

Historical Perspective

Prior to the 1800's, it was known that aphasia occurred as a consequence of various diseases of the brain, but no significant ideas about lesion characteristics had been advanced (Benton & Joynt, 1960). The early aphasia literature, as reviewed by Benton (1964) and Benton and Joynt (1960), consisted mainly of published case studies which dealt with clinical manifestations and 'psychopathologic' conceptions. The widely held associationist theory of the time suggested that aphasia was caused by an interruption in the connections between ideas and their linguistic signs. It was recognized that disease or injury to the brain caused aphasia, however, specific theories regarding

localization were absent. The early body of aphasia knowledge remained much unchanged throughout the first half of the 19th century up until the time of Paul Broca and his contemporaries.

Paul Broca's research is well known for advancing the study of aphasia in respect to localization of lesion site (Berker, Berker, & Smith, 1986). He also called attention to size of lesion as a variable related to aphasia outcome. In his report entitled "On the site of the faculty of articulated speech", Broca introduced the term "aphemie" to describe the loss of articulate speech without paralysis of the organs of articulation and without the destruction of the intellect (Berker, Berker, & Smith). He localized aphemia to the third frontal convolution and, for the first time, localized the speech center to the left hemisphere. Furthermore, Broca reported that the size of lesion "was not always in direct relation to the intensity and the impairment of language" (Berker, Berker, & Smith).

Since the time of Broca, ongoing investigation has continued in the area of localization and size of lesion. Autopsy studies of lesion location and extent in the 1940's were typically based on young, army veterans with traumatic etiology (Eisenson, 1947; Eisenson, 1949). Based on his autopsy studies, Eisenson concluded that no reliable correlation could be made between type of language dysfunction and site of brain injury. He also deduced that there was no consistent relationship between the extent of brain injury and the capacity to relearn language.

During the 1950's, the study of the brain advanced from trauma cases with autopsy follow-up to in-vivo studies using electrical stimulation techniques. Wilder Penfield and Lamar Roberts conducted

ongoing investigations of the speech and language mechanisms of the brain with patients who were selected for operations to control cerebral seizures (Penfield & Roberts, 1959). Based on 72 patients who were administered speech and language tests during electrical stimulation of the brain, the following observations were presented: (1) if the rest of the brain is functioning normally, limited excisions of any previously damaged part of the left hemisphere may be followed by only transient aphasia; (2) in order of importance for speech and language, the posterior temporo-parietal area is primary, followed by Broca's area, and the supplementary motor areas; and (3) persistent aphasia may occur with extensive destruction of the left hemisphere, particularly in the temporoparietal area (Penfield & Roberts).

Radioisotope brain studies were the next advancement made in the investigation of brain function. During the 1960's, Benson and colleagues conducted a series of studies using radioisotope brain scan information for localization of lesions in patients who were diagnosed as having cerebral infarction (Benson, 1967; Benson & Patten, 1967). Benson grouped his patients according to extensive examination protocols outlining ten expressive characteristics of aphasic speech. Based on his results, Benson suggested the terms 'anterior' and 'posterior' to refer to two distinct groups of patients with lesions anterior or posterior to the Fissure of Rolando. The anterior group, with lesions in the posterior-frontal cortex, had sparse output produced with distinct effort, frequent pauses, difficulty initiating sounds, disturbed rhythm, abnormal stress, dysprosodic verbalization, and abnormal pronunciation. The posterior group, with lesions

centered in the parietal or temporal areas, had speech characterized by normal rate, little or no effort, normal melody, and no problems in pronunciation but empty converstaion, and paraphasic substitutions.

In the 1970's, radioisotope studies slowly gave way to anatomical studies employing the technique of computed tomography. Since that time, CT research has had a significant impact on many aspects of the study of brain-behavior relationships in aphasia.

Computed Tomography

Recovery from Aphasia.

Beginning in 1976 to the present, brain-behavior information gained by the use of computed tomography has advanced theories in many areas of aphasia research. The earliest and most frequent topic to be studied with computed tomography has been aphasia recovery. Since 1976 numerous publications have addressed the relationship between lesion characteristics on CT and specific aspects of aphasia recovery including: (1) general recovery (Kertesz, Harlock, & Coates, 1979; Yarnell, Monroe, & Sobel, 1976); (2) recovery of auditory comprehension (Naeser, Gaddie, Palumbo, & Stiassny-Eder, submitted; Naeser, Helm-Estabrooks, Haas, Auerbach, & Srinivasan, 1987; Selnes, Knopman, Niccum, Rubens, & Larson, 1983); (3) assymetries of the brain and recovery (Pieniadz, Naeser, Koff, & Levine, 1983); (4) recovery of syntactic comprehension and production (Naeser, Palumbo, Helm-Estabrooks, Stiassny-Eder, & Albert, 1989; Tramo, Baynes, & Volpe, 1988); (5) the value of acute CT in recovery predictions (Murdoch, Afford, Ling, & Ganguley, 1986); and (6) recovery from subcortical aphasias (Fromm, Holland, Swindell, & Reinmuth, 1985).

The aphasia results reported by the researchers for their studies were fairly straightforward. The results of these studies revealed that: (1) size, location, and number of lesions on CT had a good correlation with aphasia outcome (Yarnell et al., 1976); (2) lesion volume, except where very large or very small, was not closely associated with outcome (Selnes et al., 1983); (3) lesion size correlated specifically with recovery of comprehension (Kertesz et al., 1979); (4) there was a highly significant correlation between recovery of comprehension and the amount of temporal lobe lesion in Wernicke's area but no significant correlation between recovery of comprehension and total temporoparietal lesion size (Naeser, Helm-Estabrooks, et al., 1987); (5) atypical occipital asymmetries were significantly associated with certain aspects of language recovery (naming, single-word comprehension, and single word repetition) (Pieniadz et al., 1983); (6) persistent deficits in syntactic manipulations are associated with anterior perisylvian lesions (Tramo et al., 1988); (7) acute CT scans have only limited value in aiding the formulation of a prognosis for aphasia recovery (Murdoch et al., 1986); (8) language skills recover more rapidly and completely than do cognitive skills in subcortical lesions and recovery was most dramatic within the first six to eight weeks after onset (Fromm et al., 1985); (9) there is a significant difference in recovery of auditory comprehension in global aphasia for lesions in Wernicke's cortical area as compared to subcortical temporal lobe lesions (Naeser et al., submitted); and (10) lesion extent in subcortical white matter areas are relevant in predicting potential for recovery of spontaneous speech (Naeser et al., 1989).

Traditional Aphasia Classification. The second most frequent topic in the area of aphasia to be studied with the use of computed tomography brain imaging is localization of lesion. Early research, employing young generations of CT technology, tended to conclude that there was a good correlation between lesion location and aphasia type based on Geschwind's Localization Theory, and subsequently the Boston Diagnostic Aphasia Examination (Goodglass & Kaplan, 1972) (Hayward, Naeser, & Zatz, 1977; Naeser & Hayward, 1978; Naeser, Hayward, Laughlin, & Zatz, 1981).

Later studies began to suggest that although some CT lesion localizations were compatible with the traditional views of aphasia classifications, there was not a one-to-one relationship between specific aphasic syndromes and particular regions within the language area (Basso, Capitani, Laiacona, & Zanobio, 1985; Basso, Lecours, Moraschini, & Vanier, 1985; Mazzocchi & Vignolo, 1979; Vignolo, 1984; Vignolo, Boccardi, & Caverni, 1986; Poeck, de Bleser, & von Keyserlingk, 1984).

Exceptions to the Localization Theory were illustrated by patients who demonstrated: fluent aphasia with anterior lesions and nonfluent aphasia with posterior lesions (Basso, Lecours et al., 1985); purely anterior or posterior lesions in global aphasia, or, purely deep lesions in Broca's aphasia (Mazzocchi & Vignolo, 1979; Vignolo et al., 1986); regions in the left hemisphere outside of the classic areas of Broca and Wernicke which were associated with aphasia (Vignolo, 1984); and crossed-aphasia in which right hemisphere lesions were associated with classic left hemisphere aphasia characteristics (Basso, Capitani et al., 1985).

Subcortical Lesion Sites and Aphasia. Beginning in the early 1980's, attention began to focus on noncortical lesions which had an effect on speech and language after stroke. Researchers suggested that: lesions involving the anterior limb of the internal capsule, the head of the caudate, and the putamen in the left hemisphere demonstrated aphasia (Damasio, Damasio, Rizzo, Varney, & Gersh, 1982); subcortical infarctions with basal ganglia involvement led to transient aphasia and aphasia was more severe if a cortical lesion was combined with a basal ganglia lesion (Brunner, Kornhuber, Seemuller, Suger, & Wallesch, 1982); and left basal ganglia lesions gave rise to long lasting deficits of language functions across all expressive language modalities while thalamic lesions showed impairments of speech fluency, and white matter lesions alone showed no substantial effects on language (Wallesch et al., 1983).

Most recently, the role of white matter fiber tracts within the subcortical basal ganglia region has gained attention. It has been suggested that the extent of deep white matter lesions in one direction or another of only a few millimetres can have a profound effect on the resulting language behavior (Alexander, Naeser, & Palumbo, 1987; Naeser, 1988; Naeser et al., 1982).

Magnetic Resonance Imaging

There is great potential for the use of magnetic resonance imaging in the study of aphasia (Murdoch, 1988). DeWitt et al. (1984) noted that the sylvian fissure is so clearly delineated in MRI that in-vivo anatomical localization is optimal for the study of aphasia

syndromes. DeWitt, Grek, Buonanno, Levine, & Kistler (1985) reported that CT may be inadequate in defining the extent of infarction, whereas MRI with its three planes of view demonstrates more clearly actual lesion size. Caplan and DeWitt (1988) recently reported that MRI is superior to CT in demonstrating acute and chronic ischemic infarction and suggest the use of MR brain imaging as the technique to determine the localization of aphasia types. Murdoch (1988) delineates additional advantages MRI has as compared to CT in stroke management, including: its ability to distinguish gray and white matter, its sensitivity to early changes associated with stroke, and its lack of boney artifacts.

At this stage in its clinical development magnetic resonance imaging has yet to be used extensively in the field of aphasiology (Albert & Helm-Estabrooks, 1988; Murdoch, 1988). As did the other brain imaging techniques, magnetic resonance imaging is slowly entering the field. Three case study research reports have recently been published in regard to the localization of lesions on MRI and their correlation with aphasia (DeWitt, Grek, Buonanno, Levine, & Kistler, 1985; Poncet, Habib, & Robillard, 1987; Tranel, Biller, Damasio, Adams & Cornell, 1987). Typical of a period of transition, the research cases report both CT and MRI results.

DeWitt et al. (1985) describe two case reports of patients with aphasia resulting from stroke. Both patients received CT and MR imaging studies, with MRI images collected at a plane corresponding to CT. For Subject 1, a CT scan collected within 24 hours of stroke demonstrated an infarction located subcortically involving the left caudate, internal capsule, and lenticular nucleus. MRI showed a large

area of involvement occupying the entire fronto-insulo-temporal cortex in addition to medial extension into subcortical white matter, basal ganglia, and internal capsule.

Subject 2, in the DeWitt et al. (1985) study demonstrated a small infarction involving the left posterior temporal cortex and adjacent white matter on CT. MRI demonstrated a greater anteroposterior extension of the infarct when compared with CT. Both imaging studies were completed at the time of infarct.

Poncet et al. (1986) report one case of sudden onset of conduction aphasia in a 70 year old male. Six days poststroke, a CT scan demonstrated a questionable deep parietal hypodense area. Two months postonset, an MRI scan demonstrated a well circumscribed lesion in the deep left parietal white matter, near the insula, and posterior and superior to the lenticular nucleus.

Tranel et al. (1987) report three cases of acute onset of global aphasia without accompanying right hemiparesis. The results of brain imaging studies confirmed discrete lesions, in both the anterior and posterior language areas for each of the subjects.

On contrast enhanced CT, six days poststroke, two well defined areas of infarction in the left hemisphere were reported for Case 1. One lesion was located anteriorly in the frontal lobe, involving the most superior part of the frontal operculum and extending into the premotor region. The other lesion was located posteriorly in the parietal lobe, involving part of the supramarginal gyrus and the inferior part of the superior parietal lobe. Five months postonset, an MRI scan demonstrated the same two lesions.

On CT obtained the day of onset, Case 2 had one lesion in the

parietal region and an ill defined area of another possible infarct in the left frontal lobe. MRI performed on the same day showed two discrete lesions, one in the frontal lobe involving the most anterior and superior portion of the frontal operculum and extending into prefrontal areas. The other lesion involved the inferior and posterior portions of the inferior parietal lobe.

On CT and MRI performed three days poststroke, Case 3 had multiple infarcts located in the left posterior temporoparietal region, left basal ganglia, left prefrontal region, right corona radiata, and right posterior occipital lobe.

CHAPTER III

Methods

Goal of the Study

The goal of this retrospective study was to investigate, quantitatively, lesion size and location in occlusive stroke as demonstrated by the brain imaging techniques of computed tomography and magnetic resonance imaging. This chapter describes the procedures that were used to achieve this goal.

Subjects and Subject Selection Process

Subjects

Data from ten adults, above the age of 20 years, was analyzed in the present investigation. Twenty years was selected as the minimum age for subject inclusion as it is the approximate age at which the brain has reached its full adult weight and no longer continues to grow in size (Brody, 1985). This minimum age criterion was desirable in order that any variations in brain anatomy during growth and development, which may be visualized by brain imaging techniques, did not interfere with the goal of the study. Subjects had a single occlusive cerebrovascular accident either in the left or right hemisphere as demonstrated on computed tomography (CT). CT imaging

was done in the patient's respective hospital or clinic during the acute to subacute stage post stroke, ie. up to 21 days postonset. Subsequent to their CT, a follow-up magnetic resonance imaging (MRI) study done in the Department of Radiology, Michigan State University confirmed the diagnosis of occlusive infarct. The follow-up MRI studies were prescribed by the referring physician either to gain additional information pertaining to the diagnosis of stroke or to aid in a differential diagnosis. Five of the final ten subjects were referred for an MR scan specifically to rule out an infarct after an abnormal CT was found. Another four of the final ten subjects were referred for an MR scan because their CT was abnormal and the MR would provide additional information. The last subject was referred for the purpose of a differential diagnosis between tumor and stroke.

The aging of an occlusive infarct on neuroimaging is a continuous process, but in general the first few days to a week after a stroke is called the acute stage poststroke, the next couple of weeks is called the subacute stage, and after approximately the third week the chronic stage begins (Adams & Sidman, 1968). This study was based on brain image data obtained during the early weeks poststroke in order to allow generalization of the results to information typically gathered from brain images acquired in the early medical management phase. All CT and MRI studies were done within 37 days poststroke. For the ten subjects, CT imaging was done between one and 21 days post stroke with a mean of 6.3 days. MR imaging was done between three days and 37 days with a mean of 18.6 days. The time between CT and MR imaging studies ranged from two days to 36 days, with a mean of 12.3 days. All CT and MRI data for this study was collected retrospectively.

Information pertaining to hypertension and/or diabetes was obtained at the time of the MRI scan as part of the patient's medical history and was noted for this study. This information was collected due to the additional effects these conditions may have on the brain. Animal studies have found that hypertension and/or diabetes are associated with an increased size of infarct in stroke (Duverger & MacKenzie, 1988). One hypothesis for this finding is that hypertension and/or diabetes exacerbates the brain edema that accompanies the infarct (Duverger & MacKenzie). The increased severity of brain edema may cause the lesion to be larger in size. MRI has been shown to demonstrate edema more effectively than CT (Bradley, 1987; Naruse & Hirakawa, 1986). If a history of hypertension and/or diabetes makes the edema surrounding an infarct more pronounced, the lesion may actually look larger on MRI than CT. No other medical conditions which would have influenced the results of this research were evident from the medical histories of the ten subjects.

All subject data collected in this investigation was identified by number without reference to individual participants in order to ensure confidentiality. A summary of subject characteristics listing age, gender, time postonset for computed tomography, time postonset for magnetic resonance imaging, and medical history of hypertension and diabetes can be found in Table 1.

Table 1

Subject Characteristics

Subject	Age in Years	Sex	Days post stroke CT imaging	Days post stroke MRI imaging	Medical History
1	60	M	3	10	-
2	44	M	4	7	D
3	53	M	7	14	-
4	27	M	1	3	-
5	27	F	8	30	-
6	49	F	11	14	D, H
7	31	M	6	14	-
8	66	M	21	36	-
9	50	M	1	37	H
10	45	F	1	21	-
$\bar{X}$	45.2		6.3	18.6	

D = Diabetes, H = Hypertension, - = no medical history of diabetes or hypertension.

Subject Selection Process

A representative of the Department of Radiology at Michigan State University was given a description of the subject criteria for this study. The radiology representative reviewed patient files of persons who had been referred for magnetic resonance imaging scans between June 1985 and February 1988. All patients above the age of 20 who had been referred for an MRI study because of a previously abnormal CT study or specifically for the reason of ruling out an infarct were identified from the radiology files. Only those patients who had a previous CT study and had a confirmed occlusive stroke on MR imaging were considered as possible subjects for the study. Those who had both CT and MRI scans completed within 37 days of stroke, and who were later during this study determined to have had only a single lesion in either hemisphere on CT, comprised the final subject population. CT imaging was done in the patient's respective hospital or clinic. In order to obtain copies of the patient's CT scans, a radiology representative from Michigan State University contacted the patient's referring hospital by telephone and requested the x-ray department send copies of the patient's CT scan to MSU.

Experimental Procedures

Computed Tomography

The computed tomography images for the subjects used in this study had been completed on a variety of models of CT scanner depending on the location of the acute hospitalization of the patient.

All scanners were the latest generation equipment. Control settings such as window width, window center and slice thickness were therefore independently determined for each CT study. Window width refers to the range of x-ray absorption values, or the sensitivity setting, selected for a particular study (de Groot, 1984; Koehler, Anderson, & Baxter, 1979). Window center refers to the center of that segment of the total scale of absorption values (Koehler, Anderson, & Baxter.) The settings chosen for a particular study determined which portion of the total range of CT values were included in the image being viewed. The settings selected have an influence on the extent of the boundaries of an area of pathology (Koehler, Anderson, & Baxter). Optimal settings for best visualization of pathology vary with different scanner models (Weisberg, Nice & Katz, 1984). Generally, since tissue densities in the brain fall within a narrow range, control settings for a brain study are chosen in a standard fashion (Koehler, Anderson, & Baxter). Window width settings of 80 to 150 Hounsfield units are usually used for routine scans of the brain (de Groot, 1984).

Information pertaining to the type of CT machine, window width settings, and slice thicknesses for each of the individual CT examinations included in this study is summarized in Table 2. All studies used contiguous image slices. Only CT images completed with contrast enhancement were included in this study to control for any increased visualization of lesion extent in images taken with, as opposed to without, contrast injection. It has been reported that contrast enhancement generally increases the density of infarcts and therefore their visibility on CT (Zulch, 1985).

Table 2

Parameters of the Contrast Enhanced Computed Tomography (CT) Studies Collected Retrospectively

Subject	Type of CT Machine	Window Width Setting	Slice Thickness
1	GE - CT/T	250	10.0 mm
2	Siemens SOMATOM DR	112	8.0 mm
3	Picker INTL SE	68	8.0 mm
4	Philips TOMOSCAN 310	150	9.0 mm
5	Philips TOMOSCAN 300	76	9.0 mm
6	Technicare Delta 2060	138	10.0 mm
7	Philips TOMOSCAN 310	100	9.0 mm
8	GE - CT 9800	80	10.0 mm
9	Philips TOMOSCAN 310	150	9.0 mm
10	Technicare DELTA 2060	127	10.0 mm

Magnetic Resonance Imaging

Subsequent to their CT study in their respective hospitals, all subjects had been seen for a magnetic resonance imaging study in the Department of Radiology, Michigan State University. Subjects had their MRI study completed after their CT study and no more than 37 days poststroke. (Please see Table 1 for individual subject data.) All MRI images were obtained on a 1.5 Tesla General Electric Signa Magnetic Resonance System. Tesla refers to the unit of magnetic field density used in MR imaging. One Tesla (T) is equal to 10,000 gauss or 10,000 times the approximate strength of the earth's magnetic field on its surface (Elster, 1986).

There are numerous imaging parameters which must be specified when performing an MR scan in order to obtain optimum results (Elster, 1986; Wehrli & Field-Quick, 1988). Changing the combination of parameter choices has an effect on the final image. The basic parameters which must be specified for an MR study include: the plane on which the brain will be pictured, the thickness of the brain slice, the size of the space between the brain slices, the size of the pieces of pictorial information and the matrix into which they fit, the size of the field of view which ultimately determines spatial resolution, the number of times information is collected from an anatomical area, and the magnetic pulse sequences and intervals.

The following imaging parameters were employed for all MRI studies included in this research. (See Table 3.) A standard number of slices, seventeen axial and seventeen sagittal, were collected. Since CT images were only obtained in the axial plane, this

correlational research between CT and MRI restricted use to the axial plane MRI images. Each axial and sagittal slice had a thickness of 5 mm and the interslice spacing distance between slices was 2.5 mm.

Each square of pictorial information is called a pixel (picture element) and may range from black to white through 64 shades of darkness (General Electric, 1984). An acquisition matrix of 256 X 128, which was used in this study, indicates that a grid of 256 squares of pictorial information (pixels) by 128 pixels was computer processed and displayed in each image. Studies were done with a field of view (FOV) of 24cm. At a given matrix size, field of view determines pixel size and therefore spatial resolution (Wehrli & Field-Quick, 1988). At a FOV of 24cm and matrix size of 256 X 128, the pixel size was 0.9mm X 1.9mm (Elster, 1988). Nexus refers to the number of exitations (NEX) or number of times information was collected from the same anatomical area in order to improve the signal-to-noise ratio and therefore the resolution of an image (Wehrli & Field-Quick). By repeated sampling, the signal-to-noise ratio is improved. The MRI images in this study were done at a nexus of 2.

Two images were made of each anatomical slice, representing 1st and 2nd echo of the spin echo pulse sequence technique. The spin echo pulse sequence is the most common of all magnet pulse sequences used in medical imaging applications (Wehrli & Field-Quick, 1988) and is standard at Michigan State University. The pulse timing parameters of repetition time (TR) and echo time (TE) are common to all pulse sequences. Magnet pulse parameters of TR of 2000 and TE of 40 (1st echo) and 80 (2nd echo) were used for the spin echo sequences. Repetition time or TR refers to the period of time between the

beginning of a magnetic pulse sequence and the beginning of the next pulse sequence. TE refers to the echo time, or the time between the beginning of the magnetic pulse and the detection of the emitted signal.

Table 3

Parameters of the Magnetic Resonance Imaging (MRI) Studies Collected Retrospectively

Parameter	Option Employed in all MRI Studies
System	1.5 Tesla General Electric Signa System
Plane of Image	Axial
Slice Thickness	5 millimeters
Interslice Space	2.5 millimeters
Acquisition Matrix Size	256 X 128 Pixels
Field of View (FOV)	24 centimeters
Number of Excitations (NEX)	2
Pulse Sequence	Spin Echo
Pulse Time Intervals	Repetition Time (TR) = 2000
	Echo Time (TE) = 40, 80

Data Collection

Data from the computed tomography and magnetic resonance images were collected in a retrospective fashion. The CT images were collected from the respective hospitals and clinics around the state of Michigan at which the patients had their acute medical management. The MRI images were collected from the files of the Department of Radiology at Michigan State University.

Three radiologists were engaged to 'read' and make measurements from the CT and MRI images. The same three radiologists were used throughout the data collection and worked independently of each other for all analyses. Radiologist A had 8 years training and experience with brain computed tomography images and 3.5 years with brain magnetic resonance images. Radiologist B had 6 years training and experience with brain CT images and 3 years with brain MRI images. Radiologist C had 3 years training and experience with brain CT images and 2 years with brain MRI images. It has been reported that interpretation of pictographic data depends on visual search strategies (Kundel & La Follette, 1972). The evolution of visual patterns, demonstrated by eye movements made while looking at an image, occurs during medical school and changes very little beyond residency training. The development of visual search strategies, however, depends more on knowledge of radiographic anatomy and pathology (Kundel & La Follette).

The procedure followed by each radiologist for each of the ten subjects is described in detail below. To control for fatigue, radiologists completed the following procedure for five subjects at a time. The ten subjects therefore, were completed in two sessions per

radiologist. An additional third session for each radiologist allowed for repeated measurements on cases used for reliability. (See reliability section.)

Determining Single Lesion on CT. The three radiologists viewed the CT images for each potential subject to identify if there was any pathology on the CT films. Only the patients who were identified by all radiologists to have a single lesion in either hemisphere on CT were included in the study. Patients identified by any one radiologist to have a normal CT scan or more than one lesion on CT were eliminated from the study. Ten subjects passed this single lesion criterion and were included in the final subject pool.

Choosing the Images for Study. For the ten patients identified to have a single lesion in either hemisphere on CT, the three radiologists independently identified all of the CT image slices in which the lesion appeared. For the same patients, the three radiologists individually identified all of the MR image slices in which the same target lesion appeared.

When identifying the image slices in which the lesion appeared on the two modalities, the three radiologists may or may not have chosen the same images. For example, for subject one, the three radiologists all individually identified the lesion to appear on CT slices 2, 3, 4, 5, and 6 and MRI slices 15, 17, and 19. For subject 2 however, on CT, radiologists A and B chose image 17 and radiologist C chose images 17 and 18 to depict the lesion. On MRI, all three radiologists chose images 23 through 27 to depict the lesion. The primary investigator recorded the image numbers chosen by each radiologist to depict the lesion on CT and MRI to allow future comparison between radiologists.

At this point in the study, CT images and MRI images were separated and randomized. All future data collection was done independently for CT scans and MRI scans for each subject. In this way, the radiologists were unaware of the corresponding lesion on the two modalities. It has been suggested that when two imaging procedures are being compared, the ideal experiment includes randomization of the order of presentation of the images in order that results from the imaging procedure of comparison is unknown, and 'blinding' of the observer to the patient's clinical history (Cooper, Chalmers, McCally, Berrier, & Sacks, 1988). In this study, both of these conditions existed. The CT and MRI images were presented to the radiologist observers in a randomized fashion with no comparison possible for the same lesion between the two modalities. The radiologists were also unaware of any medical or clinical history for the ten subjects, except that they had been preselected for the study on the basis of possibly having a stroke.

At the time when the radiologists first inspected the CT and MRI studies for each subject, head symmetry was noted to inspect for head tilt. On MRI, the radiologists noted the location of the lenses of both eyes of the patient to confirm that they appeared at the same axial level. On CT, the radiologists confirmed that the ventricles were symmetrically seen at the same axial slice level. There was no head tilt identified for any of the ten subjects included in this study that would have influenced lesion size or location data.

Outlining the Boundary of the Lesion. The three radiologists outlined the boundary of the target lesion on all CT images and on all MRI images for the ten subjects. CT and MRI images were randomized in

their presentation. Radiologists were instructed to outline the full extent of the lesion including any reversible damage such as edema and to put the outline on the very outside border of the lesion boundary in order to capture the full extent of the damage. The outlining was done using a superfine permanent Stabilo 196P overhead projector pen on a clear overhead transparency placed on the actual image. Each transparency was labelled with identification information regarding imaging modality (CT or MRI), subject ID code and radiologist ID code. (See Appendix A.) An overall study code was also assigned each transparency. This study code was necessary in order to ensure complete anonymity when the transparency outlines were copied for measurement collection. The code was also later used by the primary investigator for image identification.

Collecting Anatomical Lesion Location Data. In order to collect data pertaining to anatomical lesion location, a list of 28 brain structures was prepared. (Please see Appendix B.) The list of brain structures included 27 distinct primary anatomical brain areas. The 28th brain area, lenticular nucleus, was listed separately but also repeated more specifically as the two individual areas globus pallidus and putamen. No other anatomical area was reduplicated on the checklist. Based on the area included in their outline of the lesion on CT or MRI, the three radiologists independently reported to the primary investigator which of the anatomical structures on the list were affected by the lesion. (Lenticular nucleus was only used in localization of a lesion when location could not be more specified to globus pallidus and/or putamen.) This localization procedure was followed for all ten CT and MRI studies. Only the localization data

which was consistent between at least two radiologists was eventually highlighted in the data analysis.

In addition to localizing the target lesion for each subject, the radiologists were also asked at this time to report any other comments which they would have made regarding the brain if the scans were being read in a routine fashion. Since subjects for the study were chosen based on a single lesion on CT, this additional request was relevant only to MRI scans. The additional information; such as other brain lesions, or white matter changes indicative of aging effects were subsequently used in a supplementary analysis.

Collecting Lesion Size Data. In order to begin to calculate size of target lesion, the surface area of the lesion in each axial slice in which the lesion appeared was determined. These pieces of area were added together and then multiplied by slice thickness which resulted in an overall determination of lesion volume. This procedure was employed for computed tomography and magnetic resonance images.

Specifically, to determine lesion surface area, a grid method of measurement was employed. The outlined lesions on transparencies (see Appendix C) were copied directly onto grid paper using a Xerox 1065 Copier (see Appendix D). One grid page was used for each lesion as outlined on either CT or MRI. Multiple outlined areas were copied onto one grid page if a single lesion appeared in more than one CT or MRI image slice. The grid pages were composed of squares 1/20th of an inch in size. The grid pages did not contain any identifying information as to the modality of imaging, corresponding image, subject code, or radiologist code. An overall study code was assigned to each grid page which was later used for image identification by the

primary investigator.

Two nonradiologists served as lesion size judges for the study. These judges calculated lesion surface area using the grid method for each of the outlined lesions of the CT and MRI images. Each judge was trained independently at a training session which lasted approximately 30 minutes. At the training session, each judge was given an instruction sheet which explained the exact procedure to use for determining lesion size. (Please see Appendix E.) Using a sample lesion, the investigator demonstrated the grid method of measurement. Specifically, the judges were trained to determine surface area of the lesions by counting the number of squares contained within the lesion. All boxes counted and included within the lesion area were marked with a dot from a thinline marker. A box was included if half or more of the square was within the outline. The actual boundary of the lesion outline was not considered to be part of the lesion and therefore not included in the area measurement. If the boundary outline was thicker/thinner in some parts of the lesion than others (this occurred in one outlined portion of one lesion; Radiologist A, subject 10, MRI) or if the outline was not completely closed around the lesion (this occurred in one outlined portion of one lesion; Radiologist A, subject 6, MRI), the lesion size judges were told to assume the line was the same thickness around the total area of the lesion and to assume the closure of the line. Totals for each outlined area were noted at the side of the respective area. (See Appendix F.)

During the training session, the judges each duplicated the measurement technique illustrated by the primary investigator with a sample lesion and then demonstrated proficiency with the measurement

technique on two additional sample outlined lesions. This sample data was not included in the actual study. After the judges demonstrated proficiency by duplicating the measurement technique on three lesions, the investigator distributed approximately half of the 84 grid sheets with outlined lesions to each judge to complete independently on their own time. There was no time limit imposed for completing the measurements.

Judge 1 was trained approximately two weeks prior to Judge 2. After the initial training of Judge 1, additional questions regarding the measurement technique were answered by telephone. These additional guidelines were subsequently incorporated into the training of Judge 2 at the initial training session. (See Appendix G.)

When the judges completed their measurements of the first set of grid pages, they were each given the second half of the grid sheets to complete in the same manner. In total, each judge completed 84 grid pages which included CT and MRI lesion outlines for each of the ten subjects done by three radiologists, plus 24 additional pages for reliability checks (please see reliability section).

When all of the completed grid pages were returned, the total surface area (number of blackened boxes) was then summed by the primary investigator for each lesion on each grid page (see Appendix H). Appendix I lists all of the raw data collected from the completed grid pages. It summarizes the surface area, in number of grid boxes, as calculated by Judge 1 and Judge 2 from the outlines of CT and MRI lesions for ten subjects as done by all three of the radiologists.

Calculating Lesion Area. After the two judges completed their independent calculations of the surface areas, there were two sets of judgements for each outlined lesion. Furthermore, since three radiologists outlined the same lesions, there were in total six surface area determinations for each lesion on CT and on MRI. (See Appendix I).

In order to decrease the effect of individual measurement error across radiologists, and to eliminate some of the interjudge variation in the radiologists' determination of lesion size, a deviation statistical procedure was employed (Grubbs & Beck, 1972). The goal of this procedure was to eliminate the most outlying measurements of lesion size and then average the remaining measurements of lesion size to result in one determination of lesion area. The critical value for exclusion as an outlier with three judges is 1.155 at the .01 level (Grubbs & Beck). Any measurement which is more than the critical value of 1.155 from the other two measurements is considered an outlier. According to this statistical procedure, Radiologist A was determined to be an outlier on his measurement of lesion area with CT in seven of the ten subjects. Radiologist C was determined to be an outlier on his measurement of lesion area with MRI in eight of the ten subjects. (See Appendix J for the results of the calculation of radiologist outlier.) Based on this information, size of lesion as determined by Radiologist A on CT and size of lesion as determined by Radiologist C on MRI was omitted from the final calculations of lesion area. Since this was a methodological study conducted to compare lesion size across the modalities of CT and MRI, the most consistent

and reliable determinations of lesion size on each of the modalities were desired to make the comparison. These most reliable judgements of lesion size were more relevant for this study than consistency of radiologists across modalities.

After omitting the outlying judgements, four data points remained for each lesion area. These four points represented two radiologists' determination of lesion area as calculated by the two lesion size judges. (See Appendix K). In the final calculation, the four data points were averaged to arrive at the final lesion surface area. This method was employed for all CT and MR images. Table 4 lists the average of the four data points for each subject for computed tomography and magnetic resonance. These averaged determinations of surface area were used in the further calculations of lesion volume for the ten subjects for each imaging modality.

Table 4

Averaged Surface Area (number of .05 inch grid boxes)

of Target Lesion on CT and MRI

	Surface Area of Lesion	
Subject	Computed Tomography	Magnetic Resonance
1	257.75	289.25
2	1.75	4.00
3	9.75	12.75
4	233.50	901.75
5	6.75	7.75
6	133.00	688.50
7	466.00	475.75
8	195.75	568.25
9	68.50	122.75
10	96.25	152.75

After establishing the surface area of the lesions on CT and MRI for each of the ten subjects, lesion volume was calculated in order to get an accurate determination of the volumetric size of the lesion. To calculate volume, information from surface area was combined with slice thickness information. Appendices L and M provide a detailed description of the procedure used to calculate lesion volume size. Appendix L pertains to CT images and Appendix M pertains to MRI images. Each step in these appendices is detailed below.

All data up to the point of determining surface area was in square inches based on 1/20th of an inch grid boxes (step 1. Appendices L and M). Surface area measurements in inches needed to be converted into square millimeters. Twenty boxes on the grid was equivalent to one inch. One inch is equivalent to 25.4 millimeters. 25.4mm squared is equal to 645.16 sq.mm. 645.16 sq.mm. divided by 400 boxes on the grid is equivalent to 1.6129 sq.mm. Therefore, 1.6129 sq.mm. multiplied by the number of boxes (N) involved on the grid resulted in a surface area measurement of the lesion in square millimeters (step 2. Appendices L and M).

All of the surface area size lesion data on both CT and MR imaging modalities was next converted to actual true life size. This conversion needed to be done for two purposes. Since the CT images used in this retrospective study were obtained from a variety of different CT systems, there was a variation in imaging protocols and magnification parameters which caused head size across CT images to differ. In order to allow comparison of lesion size across CT scans, a uniform scale of measurement was needed. All MR images were

completed on the same system, therefore head size across MR images was comparable. Head size across the modalities of CT and MRI however, differed. In order to allow comparison of lesion size across the imaging modalities of CT and MRI a comparable scale of measurement was likewise needed.

Converting lesion size to actual true life size was accomplished by multiplying surface area by a minification factor. This minification factor was a correction factor which served to counteract the reduction in size of the brain images on CT and MRI. To determine the minification factor to be used to convert the reduced image size to actual real life size for each image, the conversion scale printed on the border of the hard copy films of each CT and MRI scan was used. The conversion scale given on the image was divided by actual size measurement to result in a minification factor which would convert the reduced lesion size to actual size. This minification factor was different for each CT image and the same for each MRI image. Squaring the minification factor allowed measurements to continue in units of sq. mm (step 3. Appendices L and M). By multiplying the surface area of the lesion (from Step 2) by the square of the minification factor (from Step 3) the conversion of surface area to real size was fully achieved (step 4. Appendices L and M).

Calculating Final Lesion Volume. The final step in calculating lesion volume involved the multiplication of surface area of the lesion with the slice thickness of each image. CT image slices were contiguous, therefore only one step was necessary to arrive at the volumetric size of lesion. Lesion volume (cu.mm.) on CT was determined by multiplying the surface area of the lesion (from Step 4,

Appendix L) by the thickness of the CT slice (step 5. Appendix L). CT slice thickness varied with each subject. See Table 2 for a list of slice thicknesses per study.

MRI images are not contiguous instead slices are 5 mm thick and there is a 2.5 mm distance between slices. In order to determine volume of a lesion on MRI therefore, an estimated volume of the lesion in the interslice space needed to be added to the volume of the actual lesion from the 5mm slices. First, the actual surface area of the lesion outlined on the MR images (from Step 4, Appendix M) was multiplied by slice thickness, which was 5 mm for all MR images (step 5. Appendix M). Next, the estimated surface area of the lesion between the slices, which had been determined by taking the mean of the surface area in the two adjoining slices, was calculated (step 6. Appendix M). Steps 2 through 5, which converted actual surface area in square inches to lesion volume in cubic millimeters, were repeated with the estimated surface area from between the slices (steps 7 through 10. Appendix M). To obtain the final volume of the lesion on MRI, the direct volume determined in step 5 was added to the estimated volume between slices determined in step 10 (step 11. Appendix M).

An illustration of the calculation of lesion volume on computed tomography and magnetic resonance for Subject 1 can be found in Appendices N and O. See Table 5 for a summary of the total volume of lesion in cubic centimeters on CT and MRI for the ten subjects.

Table 5

Volume (cubic cm.) of Target Lesion on CT and MRI

	Volume of Target Lesion (cubic cm)	
Subject	Computed Tomography	Magnetic Resonance
1	28.790	30.237
2	0.221	0.418
3	1.088	1.004
4	31.125	105.876
5	0.928	0.787
6	15.255	81.183
7	49.412	38.232
8	23.062	68.428
9	9.710	13.236
10	9.703	17.078

See Appendices L through O for illustrations of the computational formula used to calculate volume of lesion

Reliability. The three radiologists independently replicated measurements for two cases of the ten (20 percent), both CT and MRI, between one and two weeks after their initial measurements. Reproducibility of results is of utmost importance when evaluating the reliability of a study (Freedman, 1987). The radiologists were unaware of their first results when repeating their observations. The two nonradiologist judges also repeated grid measurements on two cases (20 percent), both CT and MRI, between one and two weeks after completing their first measurements. They were similarly unaware of their first results on the same cases. See Appendices P and Q for the raw data of the radiologists' judgement replications and the judges' repeated calculations, respectively.

Summary

Chapter Three has presented an overview of the research procedures employed in the present investigation. Data from ten subjects, above the age of 20 years, was analyzed. All subjects had a single occlusive cerebrovascular accident in either the left or right hemisphere as demonstrated on a computed tomography (CT) study done acutely after stroke. A follow-up magnetic resonance imaging (MRI) study confirmed the diagnosis of occlusive stroke. All CT and MRI studies were done within 37 days of stroke.

Data from the CT and MRI studies was collected in a retrospective fashion. Three radiologists independently: (1) identified if there was one lesion on CT, (2) chose the CT images in which the lesion was

visualized, (3) chose the MRI axial images in which the same target lesion was visualized, (4) outlined the boundary of the CT and MRI lesion for each subject, and (5) identified affected/unaffected anatomical regions from the outlined lesions.

Two nonradiologist judges independently determined surface area of the outlined lesions using a grid method of measurement, and outlier radiologist information for size of lesion on CT and MRI was omitted. Intermediate calculations were employed to convert the averaged surface area measurement from square inches to square millimeters. Further calculations converted the data into cubic millimeters, based on CT and MRI slice thickness, to result in a final volumetric size of lesion.

Chapter Four will discuss the statistical analyses and results of this investigation.

CHAPTER IV

Results

This chapter on results includes the descriptive and statistical analyses to which the data of this study were subjected. Statistics were computed using a computer program written in Fortran Language. In all analyses, .05 alpha level was regarded as the minimal criterion for statistical significance.

The goal of this retrospective study was to investigate, quantitatively, lesion size and location in occlusive stroke as demonstrated by the brain imaging techniques of computed tomography and magnetic resonance imaging. To accomplish this objective, the three major research questions were:

1. Is there a significant difference in the number of primary area(s) of lesion involvement when comparisons are made for MRI and CT axial image measurements?

2. Is there a significant correlation between size of primary lesion for MRI and CT axial measurements?

3. Is there a significant difference between the size of primary lesions on CT and MRI?

Number of Areas of Lesion Involvement as Visualized on Computed Tomography and Magnetic Resonance Imaging

Research Question One

Studies comparing CT and MRI have suggested that MRI is the method of choice for detecting infarction (Brant-Zawadzki, 1988; Brown, Hesselink, & Rothrock, 1988; Rothrock, Lyden, Hesselink, Brown, & Healy, 1987). Occlusive infarcts are reported to be seen earlier and more clearly on MR images than on CT images (Kertesz, Black, Nicholson, & Carr, 1987; Kinkel, Kinkel, & Jacobs, 1986). Quantitative studies, however, comparing the number of specific anatomical areas of the brain affected by an infarct as visualized by the two imaging modalities have not been done. Research Question One addressed the differences between the number of areas of lesion involvement as visualized on CT and on MRI for occlusive infarcts.

Three radiologists in this study independently identified anatomical areas of the brain affected by the target lesion of ten subjects on computed tomography and magnetic resonance imaging. A checklist of 28 anatomical structures in the right and left hemisphere was employed for data collection (see Appendix B). The list of brain structures included 27 distinct primary anatomical brain areas. The 28th brain area, lenticular nucleus, was listed separately but was also repeated more specifically as the two individual areas globus pallidus and putamen. Lenticular nucleus was only reported in the localization of a lesion when location could not be more specified to globus pallidus and/or putamen. (This situation occurred with two

subjects (subjects 4 and 10) on CT and never occurred on MRI.) When lenticular nucleus was reported, it was counted as one area. When either globus pallidus or putamen was reported, each was counted as one area. If both globus pallidus and putamen were reported, they were counted as two affected areas. Lenticular nucleus was never reported or counted with globus pallidus or putamen. For each of the ten subjects, the radiologists reported which structures were affected by the target lesion on CT and on MRI.

Initially, data was collected from all three radiologists regarding which anatomic locations of the brain were effected by the target lesion on CT and MRI for each of the ten subjects. Appendix R summarizes the distribution of the three radiologist's responses with respect to the anatomic location of lesions seen on computed tomography. A combined total of 105 lesion areas were reported. Appendix S summarizes the same information for magnetic resonance imaging. A combined total of 138 lesion areas were reported.

In order to determine the most consistent number of areas of lesion involvement as visualized on each modality, only judgements of lesion location agreed upon by at least two of the three radiologists were further analyzed. Data from the areas of the brain in which only one radiologist reported involvement was omitted. These single observations could have been reported by any of the three radiologists. This elimination process was done for each anatomical area. After this refinement, a total of 85 anatomic areas of the brain were reported as involved in the target lesions for the ten subjects on computed tomography. On magnetic resonance imaging, a total of 105 areas of the brain were affected by the target lesions

for the ten subjects. See Tables 6 and 7 for this refined distribution of the radiologists' responses with respect to the anatomical location of lesions on CT and MRI, respectively.

A Student's t-test For Related Measures (Bruning & Kintz, 1968) was performed to determine the significance of the difference between the number of brain areas reported to be effected on CT and MRI for the ten subjects, after the singular radiologist observations had been omitted. The t-test result for the difference between the number of brain areas involved in the ten subjects as visualized on CT (85) and MRI (105) was not significant at the .05 level ($t = 1.76$, $p < .1$).

Although there was not a statistically significant difference in the number of total brain areas of involvement across all ten subjects, there was a trend toward more reported areas on MRI (105) than on CT (85). When the ten cases were considered individually, there were four of the ten subjects in which more anatomical areas were identified, by at least two radiologists, on MRI than on CT. In no case were more areas identified on CT than on MRI.

Table 6

Distribution of Radiologists' Responses with Respect to Anatomy of Lesions Seen on Computed Tomography Scans*

			Subjects										Totals
			1	2	3	4	5	6	7	8	9	10	
Hemisphere Lobes	Frontal	Cortex				3							3
		White				3				2			5
	Parietal	Cortex						3				2	5
		White			3			3				2	8
	Occipital	Cortex	3						3		3		9
		White	3						3		3		9
	Temporal	Cortex	3			3		2		3		2	13
		White	3			3		2		3		3	14
	Insula	Anterior								3			3
		Posterior								3			3
Deep Structures	External Capsule												0
	Claustrum												0
	Extreme Capsule												0
	Caudate	Head				3	3						6
		Body											0
	Thalamus	Anterior											0
		Pulvinar											0
	Globus Pallidus												0
	Putamen	Anterior								2			2
		Posterior											0
	Lenticular Nucleus					3							3
	Internal Capsule	Anterior				2							2
		Posterior											0
	Amygdala												0
	Corpus Callosum	Splenium											0
												Total:	85

* Singular observations have been omitted

Table 7

Distribution of Radiologists' Responses with Respect to Anatomy of Lesions Seen on Magnetic Resonance Scans*

			Subjects										Totals
			1	2	3	4	5	6	7	8	9	10	
Hemisphere Lobes	Frontal	Cortex				2							2
		White				2				2		2	6
	Parietal	Cortex				2		2					4
		White			3	2		2				2	9
	Occipital	Cortex	3					3	3		3		12
		White	3					3	3		3		12
	Temporal	Cortex	3			3				2		2	10
		White	3			3				3		2	11
	Insula	Anterior				2				3		2	7
		Posterior				2				3		2	7
Deep Structures	External Capsule									2			2
	Claustrum												0
	Extreme Capsule											2	2
	Caudate	Head					3					2	5
		Body				2							2
	Thalamus	Anterior		2									2
		Pulvinar											0
	Globus Pallidus					2							2
	Putamen	Anterior				3				2		2	7
		Posterior				3							3
	Lenticular Nucleus												0
	Internal Capsule	Anterior											0
		Posterior											0
	Amygdala												0
	Corpus Callosum	Splenium											0
												Total:	105

* Singular observations have been omitted

Reliability. Interjudge reliability measurements, for radiologists, were obtained for the number of affected brain areas reported on CT and MRI. This reliability check was done after the single reports of anatomical areas were eliminated. Reliability, as determined by the Pearson r, between Radiologists A, B, and C on computed tomography ranged from .84 to .99 ($p < .01$). Reliability on magnetic resonance imaging ranged from .84 to .92 ($p < .01$). Table 8 summarizes the interjudge correlations for the three radiologists for their reports of the number of affected brain areas on CT and MRI.

Table 8

Interjudge Reliability for Number of Affected Brain Areas Reported by Three Radiologists For CT and MRI

	Pearson r	Probability
	Computed Tomography	
Radiologists		
A and B	.84	$p < .01$
A and C	.88	$p < .01$
B and C	.99	$p < .01$
	Magnetic Resonance Imaging	
Radiologists		
A and B	.84	$p < .01$
A and C	.85	$p < .01$
B and C	.92	$p < .01$

Intrajudge reliability measures were also collected for the radiologist's own repeated observation of two subjects (subject 1 and 2) over time. Radiologists A, B, and C repeated their observations of the number of areas involved in the target lesion on CT and MRI. All observations of involved areas were included in this analysis of intrajudge comparison; single reports were not omitted. Results of this intrajudge comparison indicated that all three radiologists replicated the number of reported areas on CT for subject 1. None of the three radiologists replicated their report of number of affected areas for the same subject on MRI. For subject 2, two of the radiologists replicated their number of reported areas on CT and two of the three replicated their number of reported areas on MRI. In total, three of the six reports for subject 1 were replicated on CT and MRI. This subject's lesion was large and diffuse, and was reported to include between four to seven areas of the brain. Four of the six reports for subject 2 were replicated on CT and MRI. This lesion was small, with between one to three areas of the brain reported as involved. For the two subjects combined, five of the six CT reports were replicated and two of the six MRI reports were replicated. Table 9 summarizes the data for the intrajudge comparisons.

Table 9

Intrajudge Reliability for Number of Affected Brain Areas for Three Radiologists For CT and MRI

	Subjects			
	1	1 (repeated)	2	2 (repeated)
	Computed Tomography			
Radiologist				
A	4	4	1	1
B	6	6	1	1
C	4	4	1	2
	Magnetic Resonance Imaging			
Radiologist				
A	4	5	1	1
B	7	4	3	2
C	5	4	1	1

Size of Lesion as Visualized on Computed Tomography and Magnetic Resonance Imaging

Research Question Two

It has been suggested in the literature that the size of an infarct lesion on MRI may be larger than the size of the same lesion as visualized on CT (Duverger & MacKenzie, 1988; Murdoch, 1988). Changes in water content surrounding a lesion, referred to as brain edema, is visualized on MRI more effectively than on CT and may influence the apparent size of the resulting lesion. Research Question Two of this study specifically posed, is there a significant correlation between size of primary lesion on MRI and CT axial measurements?

Parametric Analysis. In order to answer Research Question 2, the Pearson Product-Moment Correlation Coefficient was used to determine if there was a correlation between the size of lesion on CT versus MRI. The Pearson can be used with numbers which represent amounts of measurable quantity and also assumes that the two variables are linearly related. A nonsignificant Pearson correlation of $r = .58$ ($p < .1$) was found between size of lesion on CT and size of lesion on MRI for the ten subjects. Table 5 summarizes the lesion volumes from CT and MRI which were used in the Pearson correlation.

Reliability of Radiologists' Observations. Inter- and intrajudge reliability measures for the judges' determination of lesion size based on the radiologists' tracings were determined by the Pearson Product-Moment Correlation (Williams, 1979). Pearson

correlations were determined for interjudge reliability between radiologists B and C for CT measurements and radiologists A and B for MRI measurements of lesion size. Radiologist A was eliminated from the CT reliability check and Radiologist C was eliminated from the MRI reliability check since they were determined to be outliers in their measurement of lesion size. (Refer to Appendix J.) The raw data for these correlations can be found in Appendix K. Both of these relationships were very dependable with high correlations of $r = .974$ ($p < .01$) between Radiologists B and C on CT and $r = .982$ ($p < .01$) between Radiologists A and B on MRI.

To determine intrajudge reliability, Radiologists A, B, and C replicated their measurements of lesion size for two cases (subjects 1 and 2) between one to two weeks after their initial presentation. The raw data for these repeated measurements can be found in Appendix P. Intrajudge correlations of their own repeated observations were (a) Radiologist A, $r = .992$ ($p < .01$), (b) Radiologist B, $r = .964$ ($p < .05$), and (c) Radiologist C, $r = .968$ ($p < .05$). These calculations were determined using both CT and MRI images for the two repeated cases. See Table 10 for a summary of intra- and interjudge reliability measures for the radiologists' determination of lesion size.

Table 10

Inter- and Intrajudge Reliability for Size of Lesion on CT and MRI as Determined by Three Radiologists

	Pearson r	Probability
Interjudge Reliability (Ten Subjects)		
Radiologists B and C Computed Tomography (Outlier Radiologist A omitted)	.974	$p < .01$
Radiologists A and B Magnetic Resonance (Outlier Radiologist C omitted)	.982	$p < .01$
Intrajudge Reliability (Subjects 1 and 2)		
Radiologist A	.992	$p < .01$
Radiologist B	.964	$p < .05$
Radiologist C	.968	$p < .05$

Reliability of Judges Calculations. Pearson correlations were also employed to determine the inter- and intrajudge reliability of the calculations of surface area made by Judges 1 and 2. Interjudge reliability between the two judges calculations of surface area for all ten cases on CT and MRI was very dependable at $r = .974$ ($p < .01$). Intrajudge reliability was determined for each judge's repeated calculations of surface area on two cases (subjects 1 and 5) between one and two weeks after their initial calculations. The raw data for these repeated calculations can be found in Appendix Q. The Pearson results indicate an $r = .999$ ($p < .01$), or a very dependable relationship, for both judge 1 and judge 2 repeated measurements.

Confidence of Lesion Size Results. It should be mentioned that correlational results are quite variable for small sample sizes. A single pair of values can significantly alter the overall value of the correlation. One way to demonstrate the lack of precision of correlations done with small sample sizes is to compute the confidence interval around the correlation coefficient (Kachigan, 1986; Steel & Torrie, 1980). The 95 percent confidence interval for Pearson coefficient $r = .58$ (the result of the Pearson correlation between lesion size on CT and MRI) with a subject population of ten is between (-.07 and .87). Thus, it can at most be specified that there is a 95 percent chance that the population coefficient from this small sample will fall somewhere between -.07 and .87. The width of this confidence interval clearly illustrates the lack of precision of the correlations determined with the small sample size in this study. All results should therefore be interpreted with caution.

Nonparametric Analysis. Since the relationship between lesion size using the two imaging modalities was not linear, and since the subject population for this study was less than 30, statistically it was appropriate to further analyze the data using the nonparametric Spearman Rank-Order Correlation Coefficient. The Spearman Rank-Order Correlation Coefficient (RHO) method (Ventry & Schiavetti, 1980; Williams, 1979), makes fewer assumptions about the data and specifically makes no assumptions about the shape of the relationship between the variables. It was felt that this procedure would demonstrate if a rank-order correlation existed between the CT and MRI size data, although these results would be less meaningful clinically. Results of the Spearman method, in which size of lesion on CT and MRI were rank-ordered for the ten subjects, resulted in rho = .84 ($p < .05$). (This is in comparison to the Pearson correlation of .58, $p < .1$.) See Table 11 for the list of rank-ordered size of lesion data for CT and MRI and the Spearman correlation result.

Table 11

Correlational Coefficient (rho) Between Volume (cu.cm.) of Lesion on Computed Tomography and Magnetic Resonance Imaging

	Lesion Volume (cubic cm)			
Subject	CT	Rank	MRI	Rank
1	28.790	8	30.237	6
2	0.221	1	0.418	1
3	1.088	3	1.004	3
4	31.125	9	105.876	10
5	0.928	2	0.787	2
6	15.255	6	81.183	9
7	49.412	10	38.232	7
8	23.062	7	68.428	8
9	9.710	5	13.236	4
10	9.703	4	17.078	5

	Spearman rho	Probability
CT and MRI Ten subjects	.84	$p < .05$

Figure 1 graphically depicts the relationship between volume of lesion on CT and MRI for the ten subjects. (See Table 5 for the volumetric measurements used to construct the scattergram.) From this graph, it is evident that the relationship between size of lesion on CT and size of lesion on MRI is not strongly linear. At best it can be said that there is a weak positive relationship between the size of lesion on computed tomography and magnetic resonance imaging.

VOLUME OF LESION

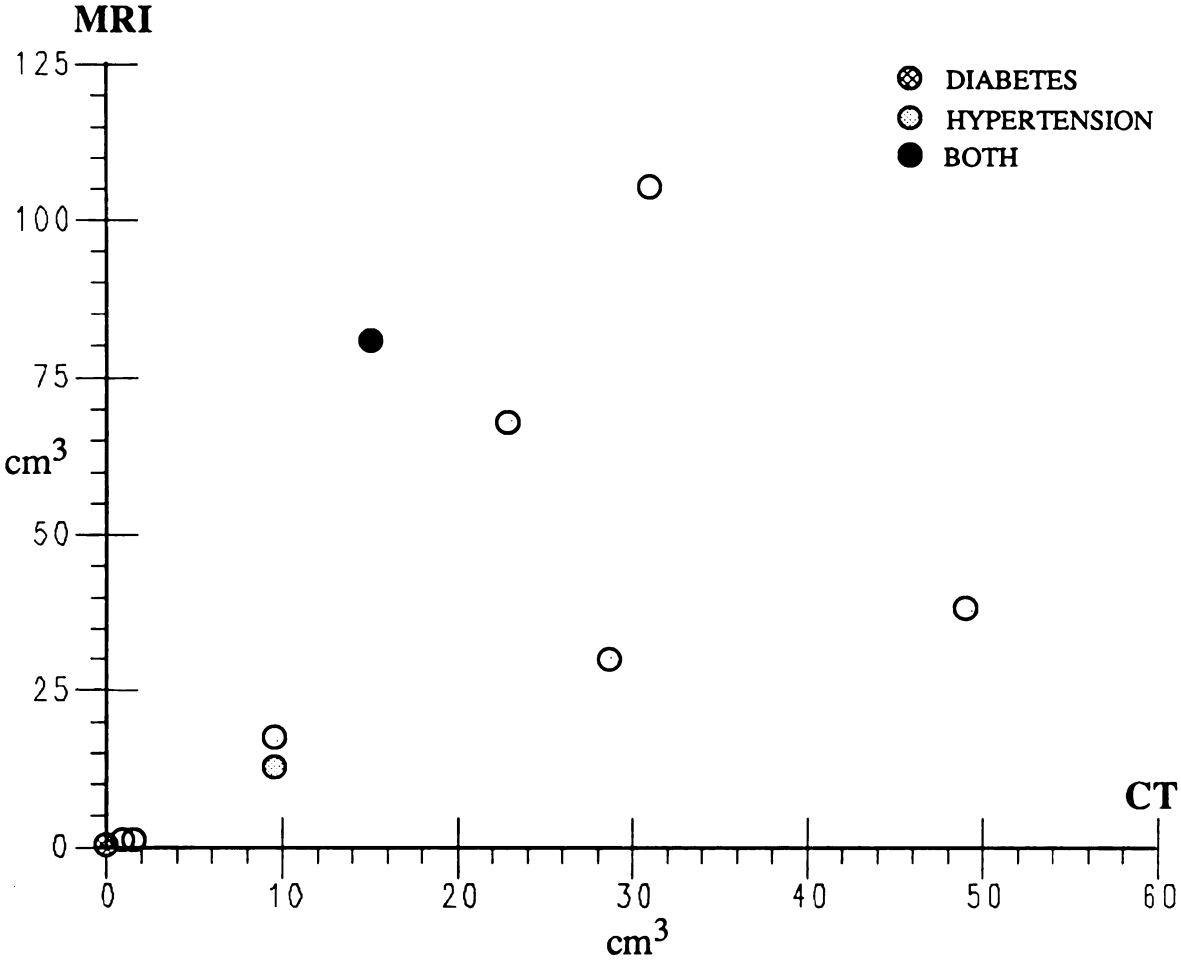

Figure 1: Scattergram depicting the relationship between volume of lesion on CT and MRI for 10 subjects

Research Question Three

As was previously discussed, it has been suggested in the literature that the size of an infarct lesion on MRI may be larger than the size of the same lesion as visualized on CT due to brain edema or changes in water content in the surrounding brain areas. Research Question Two found that there was not a significant Pearson correlation between size of lesion on CT and MRI, however the size of lesions was significantly related in a nonparametric rank-ordered analysis. Research Question Three further asked is there a significant difference between the size of lesion on CT and MRI? This analysis was done to see if lesions on MRI actually do appear larger than on CT and if so, are they significantly larger.

A Student's t-test for a difference between two independent means (Williams, 1979) was used to determine if the size of lesion on CT and the size of lesion on MRI was significantly different for the ten subjects. The mean size of lesion on MRI was 35.65 cu.cm. (SD = 35.52) and on CT was 16.93 cu.cm. (SD = 15.26). These means were not significantly different as determined by the t-test ($t = 1.453$, $p < .2$). See Table 12 for the volume measurements of lesion size on CT and MRI, and the summary statistics, used for this t-test of differences.

Although there was not a statistically significant difference in the total size of lesions across all ten subjects, there was a trend toward larger lesion size on MRI than on CT. In seven of the ten subjects (subjects 1, 2, 4, 6, 8, 9, 10), lesion volume was greater on MRI than CT. Furthermore, in three of these seven cases, the lesion

was greater than two times the size on MRI than on CT (subjects 4, 6, and 8). In comparison, the volume of lesion was larger on CT than MRI for three of the ten subjects. None of the lesions were greater than 1.3 times the size of MRI.

Table 12

Summary Statistics for Volume (cubic cm.) of Target Lesion on CT and MRI

	Volume of Target Lesion (cubic cm)	
Subject	Computed Tomography	Magnetic Resonance
1	28.790	30.237
2	0.221	0.418
3	1.088	1.004
4	31.125	105.876
5	0.928	0.787
6	15.255	81.183
7	49.412	38.232
8	23.062	68.428
9	9.710	13.236
10	9.703	17.078
Range	0.221-49.412	0.418-105.876
Mean	16.929	35.648
SD	15.259	35.524

Supplementary Analyses

Location of The Target Lesion on CT and MRI

It was found that the exact location of a target lesion was not always reported the same between CT and MRI. In five of the ten subjects, at least two radiologists reported the same areas of involvement on both CT and MRI ((a) Radiologist A, subjects 1, 3, 5, 7, and 9 (b) Radiologist B, subjects 3, 5, and 9 and (c) Radiologist C, subjects 5, 7 and 9.). The lesions which were localized to the same anatomical area(s) on CT and MRI tended to be small, in one lobe of the brain, on/or near the cortex in a general region of the brain, or in a circumscribed deep structure (ie. head of the caudate). In four additional cases, localization of the target lesion was not reported to be the same on CT and MRI by at least two radiologists. These lesions tended to be large, diffuse, located in more than one lobe, and involving cortical and/or deep structures. Appendices T, U, and V summarize the localization of the target lesions on CT and MRI as reported by radiologists A, B, and C, respectively.

One subject (subject 2) was not included in the overall comparison of localization between modalities since each of the three radiologists reported the lesion to be in a different location on CT (subcortical parietal lobe, globus pallidus, posterior limb internal capsule). On MRI the lesion was subsequently reported by two ot the three radiologists to be in a fourth location (thalamus.)

Note that in five cases (Radiologist A, subjects 2 and 8; Radiologist C, subjects 2, 4, and 6), although the number of areas

involved in the target lesion was reported the same, the actual area of the brain lesion was not reported the same.

Reliability. Agreement on complete location of target lesion, between at least two radiologists, was higher for CT than for MRI. Interjudge comparison revealed that for six of the ten subjects, (subjects 1, 3, 5, 6, 7, and 9), at least two radiologists fully agreed on the complete extent of the target lesion location on computed tomography. These lesions were located near or on the cortex, in major brain regions, or a circumscribed deep location (ie. caudate head). On magnetic resonance imaging, at least two radiologists agreed on the full extent of the target lesion for four of the ten subjects, (subjects 3, 5, 7, and 9). Single observations were not omitted for this comparison of interjudge reliability of complete lesion localization.

A complete listing of all of the areas reported to be involved in the target lesion on both modalities as reported by each of the three radiologists can be found in Appendices T, U, and V. A summary of the localization of the target lesion on CT and MRI can be found in Tables 13 and 14, respectively. At least two radiologists agreed on the complete extent of the target lesion for subjects indicated with an asterisk (*). Only the locations which were reported by at least two radiologists, however, are listed in the table. (All reports for Subject 2 on CT are included because there was no agreement between any two radiologists.)

Table 13

Location of Target Lesion as Visualized on Computed Tomography

Subject	Radiologist	Location of Target Lesion Hemisphere	
1*	ABC	Right	Temporal and occipital; cortical and subcortical
2	A	Right	Parietal; subcortical
	B		Globus Pallidus
	C		Posterior Limb Internal Capsule
3*	ABC	Left	Parietal; subcortical
4	ABC	Left	Frontal; cortical and subcortical
	ABC		Temporal; cortical and subcortical
	ABC		Caudate Head, Lenticular Nucleus
	ABC		Lenticular Nucleus
	AC		Anterior Limb Internal Capsule
5*	ABC	Left	Caudate Head
6*	ABC	Left	Parietal; cortical and subcortical
	BC		Temporal; cortical and subcortical
7*	ABC	Left	Occipital; cortical and subcortical
8	ABC	Right	Temporal; cortical and subcortical
	ABC		Insula; anterior and posterior
	BC		Frontal; subcortical
	AC		Anterior Putamen
9*	ABC	Right	Occipital; cortical and subcortical
10	ABC	Right	Temporal; subcortical
	BC		Temporal; cortical
	BC		Parietal; cortical and subcortical

Note: Only the locations reported by at least two radiologists are included above

*: At least two radiologists agreed on the complete extent of the target lesion localization

Table 14

Location of Target Lesion as Visualized on Magnetic Resonance Imaging

Subject	Radiologist	Location of Target Lesion Hemisphere	
1*	ABC	Right	Temporal and occipital; cortical and subcortical
2	AB	Right	Anterior/lateral Thalamus
3*	ABC	Left	Parietal; subcortical
4	BC	Left	Frontal; cortical and subcortical
	ABC		Temporal; cortical and subcortical
	AB		Insular Cortex
	AB		Parietal; cortical and subcortical
	BC		Caudate Body
	AB		Globus Pallidus
	ABC		Putamen
5*	ABC	Left	Caudate Head
6	ABC	Left	Occipital; cortical and subcortical
	BC		Parietal; cortical and subcortical
7*	AC	Left	Occipital; cortical and subcortical
8	BC	Right	Frontal; subcortical
	ABC		Temporal; subcortical
	AB		Temporal; cortical
	ABC		Insular Cortex
	AB		External Capsule
	AC		Anterior Putamen
9*	ABC	Right	Occipital; cortical and subcortical
10	BC	Right	Frontal; subcortical
	AB		Temporal; cortical
	BC		Temporal; subcortical
	BC		Insular Cortex
	BC		Extreme Capsule
	BC		Parietal; subcortical
	BC		Caudate Head
	AC		Anterior Putamen

Note: Only the locations reported by at least two radiologists are included above

*: At least two radiologists agreed on the complete extent of the target lesion localization

The radiologists also repeated their own observations of target lesion location for two subjects (subjects 1 and 2), between one and two weeks after their initial report. Intrajudge comparisons found that CT reports of lesion location were more frequently replicated than MRI reports. Four of the six CT reports for lesion location were replicated exactly. Radiologist A repeated both CT observations, and Radiologists B and C each repeated one CT observation. The findings for Subject 1, who had a lesion on/or near the cortex in major brain regions, were replicated three times on CT. Subject 2, with a lesion deep within the basal ganglion structures, was replicated one of the three times on CT. None of the six MRI reports for subjects 1 or 2 were exactly replicated over time for lesion location. Complete lists of the data collected during the intrajudge observations are presented in Appendices W, X, and Y.

Additional Brain Findings

During the anatomical site of lesion data collection for Research Question 1, each radiologist was further requested to make any other comments about the brain which would have been communicated in a routine radiology report. There were no additional comments made for the CT images since all subjects for this study were chosen on the basis of a single occlusive infarct on CT.

Three of the ten subjects (subjects 4, 7, and 8) had no other brain findings noted on the MRI images. Three other subjects (subjects 5, 6, and 9) had additional MRI brain findings which were only reported by one radiologist, therefore not considered for further

analysis. Of the ten subjects, four had additional brain findings on MRI as reported by at least two radiologists (subjects 1, 2, 3, and 10). As can be seen from Table 15, the additional brain findings for these four subjects were a cerebellar lesion, basal ganglion lesions, and areas of high signal intensity in the periventricular white matter, frontal and parietal deep white matter. White matter high signal intensities (HSI), which represent changes in the water content of the brain, are thought to signify either areas of demylination or small subclinical strokes (Agnoli & Feliciani, 1987; Sarpel, Chaudry, & Hindo, 1987).

Table 15

Additional Brain Findings Visualized on Magnetic Resonance Imaging Not Visualized on Computed Tomography

Subject	Radiologist	Additional Findings on MRI
*1	AB	Right cerebellar hemisphere lesion
	BC	Few small scattered HSI in periventricular/ deep white matter, bilaterally
	B	Patchy HSI in pons
*2	ABC	Left basal ganglia, 2 additional lesions (same location as target lesion on the right)
	B	Left cerebellar lesion
	C	Left pons, small HSI
*3	AC	Left frontal, small deep white matter HSI
	A	Right frontal, small deep white matter HSI
	A	Left centrum semiovale HSI, near lateral ventricle
	B	Couple of scattered HSI bilaterally
4	-	No additional findings
5	A	Right just posterior & medially to substantia nigra an old lesion
	C	Right inferior-posterior internal capsule, small lesion
6	A	Left frontal, 1 HSI centrum semiovale
7	-	No additional findings
8	-	No additional findings
9	C	Right splenium corpus callosum lesion
*10	AC	Right parietal centrum semiovale, few HSI
	C	1 midpons HSI

* = Additional brain findings confirmed by at least two radiologists
HSI = area of High Signal Intensity

Reliability. Interjudge comparison revealed that for seven of the ten subjects, there was agreement on observations of additional brain changes when only considering reports consistent between at least two radiologists. In three of these cases (subjects 4, 7, and 8), all radiologists agreed that there were no additional findings in the brain and the four other cases (subjects 1, 2, 3, and 10) were discussed above. (Please refer to Table 15.)

Intrajudge reliability measures for observations of additional brain changes were obtained for two subjects (subjects 1 and 2). All three radiologists repeated their observations for these two subjects between one and two weeks after their initial observation. Results indicate that for observations of additional brain findings on MRI, reported by at least two radiologists, there was positive replication for both subjects. Table 16 summarizes the repeated observations of additional brain findings for the two subjects by the three radiologists.

Table 16

Repeated Observations of Additional Brain Findings as Visualized on Magnetic Resonance Imaging for Two of the Ten Subjects

Subject	Radiologist	Additional Findings on MRI
1	AB	Right cerebellar hemisphere lesion
	BC	Few small scattered HSI in periventricular/ deep white matter, bilaterally
	B	Patchy HSI in pons
2	ABC	Left basal ganglia, 2 additional lesions (same location as target lesion on the right)
	B	Left cerebellar lesion
	C	Left pons, small HSI
		Replicated Observations
1	AB	Right cerebellar hemisphere lesion
	ABC	Few small scattered HSI in periventricular/ deep white matter, bilaterally
	C	2 HSI in pons
2	AB	Left basal ganglia, 2 additional lesions (same location as target lesion on the right)
	B	Left cerebellar lesion
	C	Left pons, small HSI

HSI = area of High Signal Intensity

Diabetes and Hypertension

A medical history of diabetes and/or hypertension seemed to have little influence on the overall correlation between size of lesion on CT and MRI. The original correlation between lesion size on CT and MRI with ten subjects, was not significant at $r = .58$ ($p < .1$). The Pearson correlation with eight subjects, removing the two with a medical history of diabetes (subjects 2 and 6), was $r = .61$ ($p < .2$). The Pearson with eight subjects, removing the two with a medical history of hypertension (subjects 6 and 9), was $r = .65$ ($p < .1$). Lastly, the Pearson with a total of seven patients, removing the three with a history of diabetes and/or hypertension (subjects 2, 6, and 9), was $r = .59$ ($p < .2$).

Animal studies have found that hypertension and/or diabetes is associated with an increased size of infarct (Duverger & MacKenzie, 1988). A hypothesis for this finding is that hypertension and/or diabetes exacerbates the brain edema that accompanies the infarct. MRI has been shown to demonstrate edema in the area of lesion and adjacent brain regions more effectively than CT (Bradley, 1987; Naruse & Hirakawa, 1986). This might indicate that the difference between lesion size on CT and MRI would be greater for subjects with a history of diabetes and/or hypertension. The affect of diabetes and/or hypertension on lesion size is an interesting and relevant question which should be addressed with a larger sample size. The question could not be adequately answered with the available data.

A history of diabetes and/or hypertension also did not seem to be a determining factor in the finding of additional brain changes on

MRI. Of the three subjects in this study with a medical history of diabetes and/or hypertension (subjects 2, 6, and 9), only subject 2 was reported to have additional brain findings on MRI that were not visualized on CT.

Age

In this study, age seemed to have no influence on the correlation between size of lesion on CT and MRI. The Pearson r correlation between CT lesion size and age was $r = -0.138$ ($p < .8$). The Pearson r correlation between MRI lesion size and age was $r = -0.053$ ($p > .8$). Furthermore, a partial correlation (Williams, 1979) on the relationship between size of lesion on CT and MRI with age held constant was $r = .577$ as compared to the almost identical original Pearson of $r = .578$ ($p < .1$) without holding age constant. These findings support the results of animal studies which have found no significant relationship between infarct size and age (Duverger & MacKenzie, 1988).

Age also did not seem to be a determining factor in the finding of additional brain changes on MRI. Of the four subjects with additional brain findings, two (subject 1 and 3) were above the mean age of the subject population (mean = 45.2 years) and two (subject 2 and 10) were below the mean age of the study population.

CHAPTER V

Discussion and Implications

Previous studies pertaining to brain imaging and stroke claim that magnetic resonance imaging is the method of choice over computed tomography for detecting infarction (Brant-Zawadzki, 1988; Pykett, Buonanno, Brady, & Kistler, 1983; Rothrock, Lyden, Hesselink, Brown, & Healy, 1987). Occlusive infarcts are reported to be seen earlier and more clearly on MR images than on CT images (Kertesz, Black, Nicholson, & Carr, 1987; Sipponen et al., 1983) and MRI is capable of identifying many more vascular lesions than CT (Brant-Zawadzki et al., 1985; Kinkel, Kinkel, & Jacobs, 1986). The purpose of this study was to investigate, more specifically, the comparison between lesion size and location in occlusive stroke as demonstrated by CT and MRI. To achieve this objective, CT and MRI brain imaging data from ten subjects, above the age of twenty, who had experienced stroke was analyzed retrospectively.

The results of the three main research questions of this study, comparing MRI and CT, reflect statistical nonsignificance. This nonsignificance is with regard to the comparison of occlusive lesion size, and the number of areas of lesion involvement as visualized on the two modalities in a group of ten subjects. This chapter will discuss the implications of this lack of statistical significance. In addition, trends which were observed when analyzing the subjects individually will also be discussed.

Localization of Occlusive Stroke Lesions

Results of the first research question of this study indicated that for occlusive stroke lesions in this population of ten subjects, there was not a statistically significant difference in the number of brain areas reported to be involved in the target lesion as visualized on CT versus MRI ($t = 1.76$, $p < .1$). There was, however, a trend toward more reported areas on MRI (105) than on CT (85). The lack of statistical significance may have been a consequence of small sample size (ten subjects) or the averaging effect when data across ten subjects was combined.

When analyzed individually, more anatomical areas were identified by at least two radiologists on MRI than on CT in four of the ten cases. In no case were more anatomical areas identified on CT than on MRI. Beyond simply the number of involved areas, it was furthermore discovered that in fifteen instances across five of the ten subjects (subjects 2, 4, 6, 8, and 10) a specific anatomical area was reported to be involved in the lesion by at least two radiologists on MRI but not on CT. The reverse was true, where an anatomical area was reported to be involved on CT but not on MRI, in five instances across three subjects (subjects 4, 6, and 10).

In order to examine the anatomical location of the occlusive lesions more closely, a supplementary post hoc analysis was performed on the data from question one. Anatomical locations of lesion were only considered for analysis if they were reported by at least two radiologists. If only one radiologist reported the lesion to be located in a certain anatomical location, these data were not

included. One subject was eliminated from the supplementary analysis for this reason.

For the majority of subjects (5 out of the remaining 9), the target lesion was localized to the exact same anatomical areas on CT and MRI (subjects 1, 3, 5, 7, and 9). Number of areas of lesion were therefore also the same on the two modalities. This result was found for lesions which were small, in one lobe of the brain, on or near the cortex, or in a deep structure with circumscribed boundaries. For the present data, this included lesions in the subcortical parietal lobe, cortical/subcortical occipital lobe, or the head of the caudate nucleus.

For two of the remaining four subjects (subjects 6 and 8) the two imaging modalities detected lesions in the same general regions although differences in labeling specificity were observed. This yielded a total of seven out of nine subjects for whom there were no apparent differences in actual lesion location. For the remaining two subjects (subjects 4 and 10) MRI yielded additional areas of involvement. For example; subject 4 was reported to have lesion in the parietal, cortical and subcortical regions and insular cortex on MRI but not on CT. In addition, lenticular nucleus was reported on CT, but this general description was changed to caudate body, globus pallidus, and putamen on MRI. For subject 10, frontal subcortical, insular cortex, caudate head, putamen, and extreme capsule were reported on MRI but not on CT.

It was unclear from this post hoc analysis whether differences in localization were due to labeling specificity, especially for lesions located either on the borderline of two different lobes or located

deep to the cortex in and around the basal ganglia, or due to actual differences in the detection of brain pathology by the two modalities. The clarity of CT images may also have effected the visualization of lesions on CT. Lesions in this group where localization was not the same between CT and MRI tended to be large, diffuse, located in more than one lobe, and involving deep structures. This difference in specificity contributed to the greater, although nonsignificant, number of involved lesion areas reported on MRI as compared to CT.

Implications. It has been reported that occlusive infarcts are seen more clearly on MR images than on CT images (Kertesz, Black, Nicholson, & Carr, 1987; Sipponen et al., 1983). The statistical results of this study do not confirm this observation. Nonstatistical trends of the data and analysis of individual cases, however, seem to support the notion of increased specificity on MRI.

For five of nine subjects in the present investigation (one subject was omitted from this analysis), extent and location of occlusive infarct were the same on CT and MRI. This likelihood of obtaining the same information from the two imaging modalities was greatest for lesions which were small, circumscribed within sharp boundaries, located in a general region of the brain, or located on or near the surface of the brain.

These results have particular relevance to CT research in the area of aphasia classification. The traditional aphasia classifications (Goodglass & Kaplan, 1972) are based on lesions which are cortically based and/or located in general regions in the brain. The traditional classifications include: Broca's Aphasia with a lesion involving the third frontal convolution of the left hemisphere with

subcortical and posterior extension; Wernicke's Aphasia with a lesion in the posterior portion of the first temporal gyrus of the left hemisphere; Anomic Aphasia which is associated with a lesion of the angular gyrus; Conduction Aphasia with a lesion in the arcuate fasciculus, deep to the supramarginal gyrus, or in the superior temporal gyrus; and Transcortical Sensory/Transcortical Motor Aphasias with lesions attributed to watershed regions (Goodglass & Kaplan, 1984).

Early research with CT technology has found generally good correlations between lesion location and traditional aphasia classifications (Hayward, Naeser, & Zatz, 1977; Naeser & Hayward, 1978; Naeser, Hayward, Laughlin, & Zatz, 1981). More recent research has suggested that although some CT lesion localizations are compatible with the traditional views of aphasia classifications, there is not a one-to-one relationship between specific aphasic syndromes and particular regions within the brain (Basso, Capitani, Laiacona, & Zanobio, 1985; Basso, Lecours, Moraschini & Vanier, 1985; Mazzocchi & Vignolo, 1979; Poeck, de Bleser, & von Keyserlingk, 1984; Vignolo, 1984; Vignolo, Boccardi, & Caerni, 1986). Based on the findings from the majority of subjects in the present investigation, magnetic resonance imaging studies of lesions on or near the cortex, or in general regions of the brain, would likely confirm the conclusions of previous CT research findings in aphasia studies.

Not only would MRI studies support CT research findings in regard to cortically based lesions, MRI will probably confirm CT research findings based on small subcortical lesions restricted to circumscribed areas of the brain. A lesion affecting the head of the

caudate nucleus has specifically been implicated in having an association with resulting aphasia (Damasio, Damasio, Rizzo, Varney, & Gersh, 1982). Based on the present study, the caudate head lesion would probably be reported on MRI in the same location as on CT.

Recently, numerous studies have been published which correlate subcortical lesion sites on CT with aphasia characteristics. Some of these studies have investigated gray and white matter structures such as the basal ganglia, thalamus, and internal capsule (Brunner, Kornhuber, Seemuller, Suger, & Wallesch, 1982; Damasio, Damasio, Rizzo, Varney, & Gersh, 1982; Wallesch et al., 1983) while others have specifically investigated aphasia correlations with lesions of subcortical white matter fiber tracts (Alexander, Naeser, & Palumbo, 1987; Naeser et al., 1982).

For four of the ten subjects in the present study, the location of lesion as described on CT and on MRI was not exactly the same (subjects 4, 6, 8, and 10). Furthermore, in three of these cases (subjects 4, 8, and 10), more anatomical areas of involvement were identified on MRI than on CT. MRI, with its improved resolution between gray and white matter, allowed for a more specific description of the involved areas and extent of the lesion. This increased specificity occurred with lesions which were located on the border of two different lobes or were located in deep structures in and around the basal ganglia. The findings from these subjects provide non-statistical support for radiological studies which have suggested that occlusive infarcts are seen more clearly on MR images than on CT images. Future MRI studies may not exactly replicate past CT research findings in the correlation of subcortical lesion site and aphasia for

this reason.

Size of Occlusive Lesion

In regard to the second research question of this study, there was not a direct Pearson correlation found between size of lesion as determined by CT and MR within 37 days poststroke ($r = +.58$, $p < .1$). Due to the small sample size of ten subjects however, a nonparametric Spearman correlation was further performed. This rank-ordered statistic resulted in a significant positive correlation between lesion size on the two modalities ($rho = +.84$, $p < .05$). From this data, it can be implied that for the ten subjects in this study, size of lesion on CT and MRI was positively correlated in at least a rank-order fashion.

It has been reported that MRI is particularly sensitive to changes in water content in the brain (Unger, Littlefield, & Gado, 1988). The concentration of brain water starts to change in the first hours after an ischemic event, with edemic changes continuing into the chronic stage in the evolution of the infarct (Brant-Zawadzki & Kucharczyk, 1987; Kinkel, Kinkel, & Jacobs, 1986). Although subjects for this study were scanned within the first 37 days poststroke, the range in time between stroke and imaging, and between CT and MRI, varied. Subsequently, CT and MRI scans were obtained at different times in the evolution of the infarct. This variation in time postonset, and between CT and MRI, may have influenced the correlation in size of infarct between the two modalities due to the different stages of edemic evolution.

Research question three further addressed the issue of lesion

size between the two modalities. The difference between the size of the lesion on the two imaging modalities was found to be not statistically significant ($t = 1.453$, $p < .2$). There was, however, a trend toward larger lesion size on MRI than on CT. The lack of statistical significance may have been a consequence of small sample size or the averaging effect when data across ten subjects was combined. When analyzed individually, there were seven of the ten cases in which lesion volume was greater on MRI than CT. Furthermore, in three of these cases, the lesion was greater than two times the size on MRI. In comparison, the volume of lesion was larger on CT for three of the ten subjects, and in no case was it larger than one and a third times that on MRI.

Implications. It has been reported that CT may be inadequate in defining the extent of infarction, whereas MRI more clearly demonstrates actual lesion size (DeWitt, Grek, Buonanno, Levine, & Kistler, 1985; Kinkel, Kinkel, & Jacobs, 1986). Results of the present, quantitative, study indicate that statistically, the size of lesion as visualized on CT and MRI did not differ significantly. In seven of the ten individual cases, however, lesion size was larger on MRI as compared to CT. The findings in these individual cases would support the notion that MRI more clearly demonstrated actual lesion size than CT. It must be mentioned again however that the variation in time postonset, and between CT and MR scans, may have effected the comparison of size of lesion on the two modalities. The increased sensitivity of MRI to edema, ie water changes in the brain, is particularly relevant in this regard. The stage in edemic evolution at which the CT and MR scans were obtained might have influenced the

extent of lesion.

Extent of lesion has been a frequent factor investigated in CT studies of aphasia recovery. It has been suggested that: size, among other things, has a good correlation with aphasia outcome (Yarnell, Monroe, & Sobel, 1976); lesion size correlates specifically with recovery of comprehension (Kertesz, Harlock, & Coates, 1979); amount of temporal lobe lesion correlates with recovery of comprehension in Wernicke's Aphasia (Naeser, Helm-Estabrooks, Haas, Auerbach, & Srinivasan, 1987); and lesion extent in subcortical white matter areas is important in predicting potential for recovery of spontaneous speech (Naeser, Palumbo, Helm-Estabrooks, Stiassny-Eder, & Albert, 1989).

Based on the results of the present investigation of ten subjects, lesion size found on CT may not be replicated on MRI. Conclusions regarding lesion size and aphasia recovery may, therefore, also not be replicated. If, however, it is found that there is a direct correlation between size of lesion on CT and size of lesion on MRI, the larger lesion size on MRI will be consistent across all studies and past conclusions regarding recovery will probably be confirmed. Further conclusions regarding lesion size cannot be drawn until this question is more thoroughly investigated with a larger sample population and with CT and MRI scans completed as close as possible in time to each other.

Reliability of Results

The reproducibility of results is of utmost importance when evaluating the reliability of a study. Reproducibility includes the repeated observation by the same observer over time and the measurement of interobserver variability between observers (Freedman, 1987).

In this study, inter- and intrajudge reliability of the quantitative measurement of lesion size was significant at at least the .05 level.

In regard to lesion location, results of an intrajudge reliability comparison indicated that radiologists replicated their CT observations more consistently over time than their MRI observations. The increased specificity for lesion localization on MRI may contribute to decreasing the replicability of results over time. For both modalities, lesions located in a general region of the brain were most frequently replicated. Small deep lesions, on both CT and MRI, had the lowest chance of being localized to the same area on a repeated study.

Interobserver reliability among radiologists for the localization of lesions was high for cases who had easily identifiable lesions which were small, contained within sharp boundaries, and/or were located in a general area on either CT or MRI. Reliability between observers for lesions which were deep, not contained within sharp boundaries, or large and involving more than one lobe was not as strong.

Results of the present study support the conclusions of Shinar et al. (1987), who found that agreement on localization of lesions as

visualized on CT varied widely between observers. Shinar et al. found that the level of agreement between observers rose as the anatomic category became more general. Thus, for localizing within the cerebral lobes, substantial agreement was obtained whereas in a portion of the lobe, such as the cortex or subcortical white matter, agreement declined. The researchers further found that agreement was only moderate for deep lesions in the caudate, putamen, and internal capsule and poor in the regions with 'fuzzy boundaries' such as the operculum, insula, centrum semiovale, thalamus, and corona radiata. These findings are similar to those found in the current study.

The Shinar et al. (1987) study of interjudge reliability was concerned only with computed tomography studies. Magnetic resonance imaging provides finer, more specific anatomical information than computed tomography. As would be expected, reliability of MRI anatomical reports, between observers and over time with the same observer, was found to be lower than the same reliability reports on CT. From these results it is evident that there is a need to be aware of reliability between observers and within an observer in the collection and interpretation of localization of lesion research. This caution becomes more relevant as the information becomes more precise.

The interpretation of this study's reliability results must be moderated in light of the fact that interobserver variability can only truely be assessed with a very large number of studies (Friedman, 1988).

Limitations of the Study

Subjects

The small population of ten subjects used in this study limits the interpretation and generalization of all conclusions which can be drawn from the analyses. A subject population of ten severely limits the interpretation of significance in any statistical procedure. Results should be considered preliminary observations which need to be replicated in a larger study.

The tendency, although not statistically significant, for there to be more areas of reported lesion involvement as identified on MRI compared to CT indicates a need for this question to be readdressed with a larger sample size. Likewise, the tendency, although not statistically significant, for lesions to be larger on MRI as compared to CT indicates a need for additional research. The significant nonparametric correlation between lesion size on the two modalities should be further investigated with a larger sample size and a parametric statistic.

One of the criteria established for subject selection in this study limited the subject population to people who had received CT and MRI brain imaging studies within 37 days after stroke. The number of days poststroke for CT scanning ranged from 1 day to 21 days. The number of days from CT study to MRI study ranged from 3 to 37 days. Although all of the subjects were within the early weeks of recovery, a weakness in this correlational research may be the wide range in time poststroke between the two imaging studies. Ideally, CT and MRI should be done as closely as possible in time to each other. The

variation in time poststroke may have influenced the final statistical results.

The subject population for this study was drawn from patients referred for additional MR imaging after being studied by CT. This select group of stroke patients may not represent the general stroke population.

Computed Tomography Studies

All of the MR images used in this study were obtained from the same imaging system. The study parameters for all of the images were therefore the same. In addition, original hard copy MRI prints were available for all ten subjects. In contrast, all of the CT images were obtained from different imaging systems. Study parameters (window settings; darkness and lightness) varied for each subject and copies of original CT prints were employed rather than original images. This limitation may have influenced the clarity of the CT images and therefore affected the determination of lesion localization and extent. A comparison of lesion characteristics on the two modalities should be repeated with original CT images, preferably from the same scanner, in addition to the original MRI images.

Methodology

The CT images in this study employed contiguous slices of brain images. Lesion volume on CT was determined by multiplying surface area of the lesion by slice thickness. This method assumes that a lesion is the same size in area throughout the full thickness of the slice. MRI studies, on the other hand, do not involve contiguous

slices of the brain. Each slice is 5.0 mm thick with a 2.5 mm interval between slices. Lesion volume on MRI was determined by summing together the actual measurement of surface area by slice thickness with the estimated size of lesion area by thickness between slices. This method likewise assumes that a lesion is the same size in area throughout the 5.0 mm slice. In addition, it assumes that between slices the lesion is half the size of the lesion in its adjoining slices.

The summary, conclusions, and implications for further research from the study are discussed in Chapter VI.

CHAPTER VI

Summary, Conclusions and Directions for Further Research

Summary

The purpose of this methodological study was to determine if lesion site and extent information gained by magnetic resonance imaging was comparable to lesion site and extent information gained by computed tomography. The study quantified the differences between the brain imaging techniques of CT and MRI in defining size and location of lesion in occlusive stroke. Specifically, the research questions posed were as follows:

1. Is there a significant difference in the number of primary area(s) of lesion involvement when comparisons are made for MRI and CT axial image measurements?

2. Is there a significant correlation between size of primary lesion for MRI and CT axial meeasurements?

3. Is there a significant difference between the size of lesion on CT and MRI?

Data from ten adults, above the age of 20 years, was analyzed in the present investigation. The subjects were identified to have a single occlusive cerebrovascular accident in either hemisphere on computed tomography, with a confirmed diagnosis of occlusive stroke on a follow-up magnetic resonance imaging study. Both imaging studies were completed within 37 days of stroke. Imaging results obtained during the early weeks poststroke were used in this study in order to allow generalization of the results to information typically gathered from brain images acquired in the early medical management phase. Aphasia management, including evaluation, classification, and prognostic predictions, typically occurs during these first few weeks poststroke.

Computed tomography and magnetic resonance imaging studies were analyzed in a retrospective fashion. Three radiologists confirmed the presence of a single occlusive infarct on each of the CT studies. The radiologists then chose all of the CT images in which the lesion were present and each of the corresponding MRI images in which the same target lesion was present. The radiologists outlined the boundary of the target lesion on all of the CT and MRI images and identified which anatomical structures were involved in the lesion as visualized on each modality.

Intermediate calculations determined lesion surface area size for all outlined lesions on CT and MRI. Two nonradiologist judges calculated lesion size using a grid method of measurement. These area measurements were normalized for brain size by converting to actual

size and then multiplying by brain slice thickness to conclude with a measurement of lesion volume. Lesion extent data was statistically analyzed using Pearson Product-Moment Correlation, Spearman Rank-Order Correlation, Partial Correlation, and Student's t-tests of significance. Lesion localization information was analyzed by Student's t-test For Related Measures and nonstatistical description. Intra- and interjudge reliability measures were obtained for all radiologists' observations and judges' calculations.

With respect to this study's findings, research question one was answered negatively ($p < .1$). Statistically, there were not significantly more areas of the brain affected by the target lesion as visualized on MRI as compared to CT. As evidenced in four of the ten cases, however, there was a trend for there to be more areas of involvement identified on MRI.

Research question two was also answered negatively ($p < .1$). There was not a significant correlation between MRI and CT measurements of size of primary lesion. Nonparametric Spearman Rank-Order analysis did, however, result in a significant rank-order relationship ($p < .05$) between size of lesion on CT and MRI.

With respect to research question three, the results revealed that the difference between the size of lesion on the two modalities was not statistically significant ($p < .2$). As demonstrated in seven of the ten cases, however, there was a trend for larger lesion size on MRI.

Although not included in the three research questions of this study, supplemental post hoc analysis demonstrated that lesions which were small, circumscribed within sharp boundaries, located in a

general region of the brain, and/or located on or near the surface of the brain were more likely to be localized to the same area(s) on CT and on MRI. Lesions which were large and diffuse, and/or located deep to the cortex especially in the areas surrounding and including the basal ganglia tended not to be localized to the same areas on CT and MRI. Furthermore, extent of lesion was more clearly demonstrated on MRI.

Conclusions

On the basis of the results obtained in this study of ten subjects, the following conclusions are drawn:

1. In the first few weeks after stroke, the number of reported areas of brain involvement in an occlusive lesion does not differ statistically on the two imaging modalities of CT and MRI. When analyzed on an individual case basis, there was a tendency for more areas to be identified on MRI.

2. The reported location of the lesion as visualized on CT and MRI does not differ for those which are small, in one lobe of the brain, on or near the cortex, or in a deep structure with circumscribed boundaries. MRI, however, seemed to allow for a more specific description of the involved areas of the lesion, particularly when located on the border of two different lobes or in deep structures in and around the basal ganglia.

3. In the first few weeks poststroke, there was a rank-order relationship between the size of lesions as visualized on CT and MRI. There was not a significant linear relationship between size of lesion on the two modalities.

4. There was not a statistically significant difference between the size of lesions as visualized on the two modalities. When analyzed on an individual case basis, there was a tendency for lesions to be larger on MRI.

5. The relationship between size of acute lesion on CT and MRI does not seem to be influenced by age of the patient or a history of hypertension and/or diabetes.

Directions for Further Research

The following are suggestions for continued research exploration:

1. Future studies are needed to replicate the findings in this research. Larger population sample sizes are needed to confirm the observations made in this study, increase the power of the statistical findings, and allow for generalization of results. Subgroups of patients with lesions located on or near the surface of the brain and deep to the cortex might be especially pertinent.

2. Correlational research between lesion characteristics found in brain imaging and aphasia characteristics should be conducted with

magnetic resonance imaging. This suggestion is extremely relevant to studies of lesions located deep to the cortex, in the gray and white matter in and around the basal ganglia. The ability of magnetic resonance to image in unlimited planes combined with its superiority in distinguishing gray and white matter makes this technique especially promising in the advancement of theories of brain-behavior relationships in aphasia.

3. It has been reported that the most reliable lesion size information obtainable from CT is at least six weeks to two months after stroke (Naeser, 1985; Poeck, de Bleser, & von Keyserlingk, 1984). A comparative study between imaging modalities, beyond the acute stage of recovery, would be a valuable compliment to the present study. CT and MRI studies should be done as close in time to each other as possible.

APPENDICES

APPENDIX A

SAMPLE OF TRANSPARENCY USED TO OUTLINE LESION

APPENDIX A

Sample of Transparency Used to Outline Lesion

Subject ID _____

Radiologist ID _____

CT / MRI Image # _____

Study Code _____

APPENDIX A

Sample of Transparency Used to Outline Lesion

Subject ID _____

Radiologist ID _____

CT \ MRI Image # _____

Study Code _____

APPENDIX B

ANATOMICAL CHECKLIST

APPENDIX B

Anatomical Checklist

Instructions to the Radiologist:

On the image, please notice each of the areas of the brain listed below. Check off whether the area is affected by the outlined lesion. Thank you.

RIGHT HEMISPHERE	LEFT HEMISPHERE
Frontal Lobe	Frontal Lobe
Cortical gray matter	Cortical gray matter
Subcortical white matter	Subcortical white matter
Temporal Lobe	Temporal Lobe
Cortical gray matter	Cortical gray matter
Subcortical white matter (including insular white)	Subcortical white matter (including insular white)
Insular gray matter: anterior posterior	Insular gray matter: anterior posterior
External capsule	External capsule
Claustrum	Claustrum
Extreme capsule	Extreme capsule
Parietal Lobe	Parietal Lobe
Cortical gray matter	Cortical gray matter
Subcortical white matter	Subcortical white matter
Occipital Lobe	Occipital Lobe
Cortical gray matter	Cortical gray matter
Subcortical white matter	Subcortical white matter

ANATOMICAL CHECKLIST, Continued

RIGHT HEMISPHERE

Subcortical Structures

Caudate Nucleus: Head
Body
Thalamus: Anterior/Lateral
Pulvinar
Globus Pallidus
Putamen: Anterior
Posterior
Lenticular Nucleus
Internal Capsule:
Anterior Limb
Posterior Limb
Hippocampus
Amygdala
Hypothalamus
Corpus Callosum: Genu
Splenium

LEFT HEMISPHERE

Subcortical Structures

Caudate Nucleus: Head
Body
Thalamus: Anterior/Lateral
Pulvinar
Globus Pallidus
Putamen: Anterior
Posterior
Lenticular Nucleus
Internal Capsule:
Anterior Limb
Posterior Limb
Hippocampus
Amygdala
Hypothalamus
Corpus Callosum: Genu
Splenium

Are there any other comments you would make if reading this image?

_____

_____

_____

_____

_____

APPENDIX C

ILLUSTRATION OF COMPLETED TRANSPARENCY USED IN OUTLINING LESION

APPENDIX C

Illustration of Completed Transparency Used in Outlining Lesion

Subject ID 24

Radiologist ID A

(CT) / MRI Image # 5

Study Code 58

Study Code RB

CT / MRI Image #

Radiologist ID B

Subject ID 34

APPENDIX C

Illustration of Completed Transparency Used in Outlining Lesion

APPENDIX D

ILLUSTRATION OF GRID PAGE WITH OUTLINED LESION

APPENDIX D

Illustration of Grid Page with Outlined Lesion

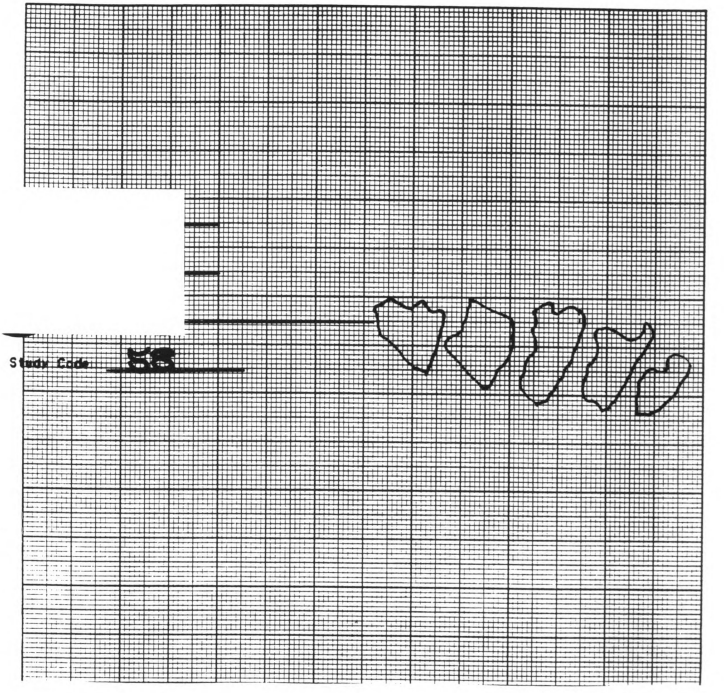

APPENDIX E

MEASUREMENT INSTRUCTION SHEET FOR RATERS

APPENDIX E

Measurement Instruction Sheet for Raters

Enclosed please find grid pages with outlined lesions copied onto the grid. The measurement you will be making is a surface area measurement of the size of the lesion. The grid is divided into 20 squares per inch. Your total area measurement will be in square inches. Follow the example below for counting the number of squares included in the outline. All boxes counted and included in the lesion area should be marked with a dot from a thinline marker. (The marker will be provided.) A box should be included if half or more of the square is within the outline. The line of the outline should NOT be included in the judgement. Totals for each outlined area should be noted at the side of the respective area. DO NOT ADD TOGETHER PIECES OF BOXES. Fill in your Judge's Code at the top of the page. Total lesion size will be summed by the primary investigator. Please follow this exact procedure for all grid pages. Thank you.

GRID PAGE _____

Judge Code _____

Total Lesion Size _____ square inches

APPENDIX F

ILLUSTRATION OF MEASUREMENT GRID

APPENDIX F

Illustration of Measurement Grid

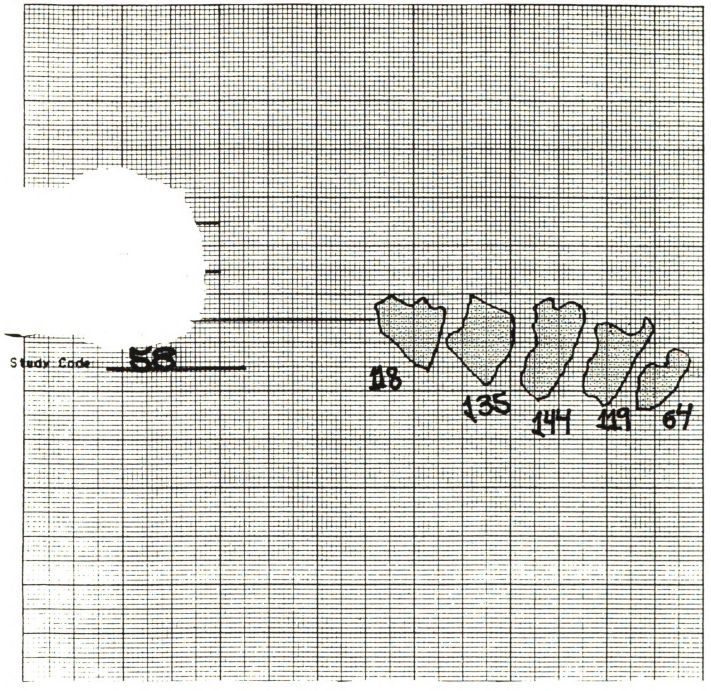

APPENDIX G

MEASUREMENT INSTRUCTION SHEET FOR RATERS, Revised

APPENDIX G

Measurement Instruction Sheet for Raters, Revised

Enclosed please find grid pages with outlined lesions copied onto the grid. The measurement you will be making is a surface area measurement of the size of the lesion. The grid is divided into 20 squares per inch. Your total area measurement will be in square inches. Follow the example below for counting the number of squares included in the outline. All boxes counted and included in the lesion area should be marked with a dot from a thinline marker. (The marker will be provided.) A box should be included if half or more of the square is within the outline. The line of the outline should NOT be included in the judgement. If the boundary outline is thicker/thinner in some parts of the lesion than others, assume the line is the same thickness around the total area of the lesion. If the outline is not completely closed around the lesion, assume the closure of the line.

Totals for each outlined area should be noted at the side of the respective area. DO NOT ADD TOGETHER PIECES OF BOXES. Fill in your Judge's Code at the top of the page. Total lesion size will be summed by the primary investigator. Please follow this exact procedure for all grid pages. Thank you.

GRID PAGE _____

Judge Code _____

Total Lesion Size _____ square inches

APPENDIX H

ILLUSTRATION OF COMPLETED MEASUREMENT GRID

APPENDIX H

Illustration of Completed Measurement Grid

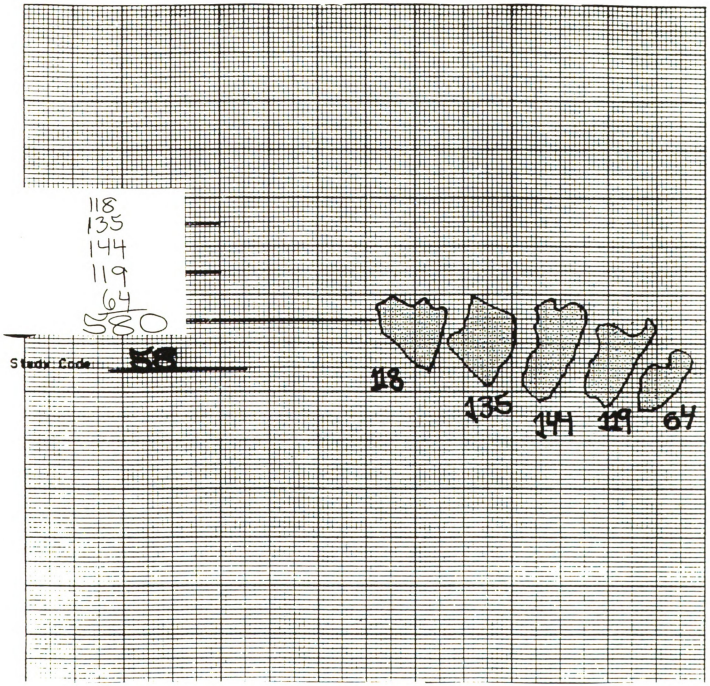

APPENDIX I

SURFACE AREA OF TARGET LESION ON CT AND MRI

AS OUTLINED BY THREE RADIOLOGISTS AND CALCULATED BY TWO JUDGES

APPENDIX I

Surface Area (number of .05 inch grid boxes) of Target Lesion on CT and MRI as Outlined by Three Radiologists and Calculated by Two Judges

		Surface Area of Lesion			
		Computed Tomography		Magnetic Resonance	
Subject	Radiologist	Judge 1	Judge 2	Judge 1	Judge 2
1	A	280	277	330	311
	B	296	292	261	255
	C	225	218	216	217
2	A	1	1	5	4
	B	3	2	4	3
	C	1	1	2	2
3	A	7	7	8	10
	B	11	13	17	16
	C	7	8	11	12
4	A	495	482	973	963
	B	270	264	844	827
	C	200	200	654	643
5	A	8	8	7	8
	B	7	6	9	7
	C	7	7	7	6
6	A	611	607	821	812
	B	175	174	563	558
	C	91	92	207	184
7	A	559	540	483	464
	B	496	494	482	474
	C	444	430	263	258
8	A	454	451	594	578
	B	233	235	554	547
	C	156	159	237	228
9	A	131	130	145	143
	B	77	78	101	102
	C	59	60	14	14
10	A	404	401	183	173
	B	150	151	126	129
	C	42	42	31	31

APPENDIX J

CALCULATION OF RADIOLOGIST OUTLIER

APPENDIX J

Calculation of Radiologist Outlier

Subject	Surface Area of Lesion (Number of .05 inch grid boxes) Radiologist A	B	C	Deviation Statistic
	Computed Tomography Imaging			
1	278.5	294.0	221.5	.444
2	1.0	2.5	1.0	.707
3	7.0	12.0	7.5	.815
4	488.5	267.0	200.0	1.379*
5	8.0	6.5	7.0	1.336*
6	609.0	174.5	91.5	1.398*
7	549.5	495.0	437.0	1.212*
8	452.5	234.0	157.5	1.369*
9	130.5	77.5	59.5	1.371*
10	402.5 (outlier)	150.5	42.0	1.352*
	Magnetic Resonance Imaging			
1	320.5	258.0	216.5	1.135
2	4.5	3.5	2.0	1.295*
3	9.0	16.5	11.5	.266
4	968.0	835.5	648.5	1.288*
5	7.5	8.0	6.5	1.331*
6	816.5	560.5	195.5	1.290*
7	473.5	478.0	260.5	1.414*
8	586.0	550.5	232.5	1.408*
9	144.0	101.5	14.0	1.340*
10	178.0	127.5	31.0 (outlier)	1.331*

* The critical value for exclusion as an outlier with three judges is 1.155 at the .01 level. Any deviation statistic more than this value confirms an outlier.

APPENDIX K

SURFACE AREA JUDGEMENTS USED IN THE DETERMINATION OF AVERAGED SURFACE AREA

APPENDIX K

Surface Area Judgements Used in the Determination of Averaged Surface Area

		Surface Area of Lesion			
		Computed Tomography*		Magnetic Resonance#	
Subject	Radiologist	Judge 1	Judge 2	Judge 1	Judge 2
1	A			330	311
	B	296	292	261	255
	C	225	218		
2	A			5	4
	B	3	2	4	3
	C	1	1		
3	A			8	10
	B	11	13	17	16
	C	7	8		
4	A			973	963
	B	270	264	844	827
	C	200	200		
5	A			7	8
	B	7	6	9	7
	C	7	7		
6	A			821	812
	B	175	174	563	558
	C	91	92		
7	A			483	464
	B	496	494	482	474
	C	444	430		
8	A			594	578
	B	233	235	554	547
	C	156	159		
9	A			145	143
	B	77	78	101	102
	C	59	60		
10	A			183	173
	B	150	151	126	129
	C	42	42		

* Outlier Radiologist A omitted
# Outlier Radiologist C omitted

APPENDIX L

DESCRIPTION OF CALCULATION OF LESION VOLUME ON COMPUTED TOMOGRAPHY

APPENDIX L

Description of Calculation of Lesion Volume on Computed Tomography

---

1. The total number of .05 inch grid boxes for the subject was determined.

---

2. The total number of .05 inch grid boxes was converted into square millimeters to result in a surface area measurement.

   20 grid boxes = 1 inch
   1 inch = 25.4 millimeters
   25.4 mm x 25.4 mm = 645.16 sq.mm
   20 boxes x 20 boxes = 400 boxes

   (25.4 mm / 20) x (25.4 mm / 20) = (645.16 sq.mm / 400) = 1.6129 sq.mm

   [Total number of boxes] x [1.6129 sq. mm] = Surface Area in sq.mm

---

3. In order to allow comparison of lesion size across images and modalities, all measurements were converted to real size. Thus, to counteract for the reduction in size on the images, a correction factor was determined for each image. This correction factor was called a minification factor and was determined by using the conversion scale provided on each image. This factor was squared in order to use in the calculations which followed.

   [CT conversion scale measurement (mm)] / [Actual size measurement (mm)] = Minification Factor

   [Minification Factor] x [Minification Factor] = Minification Factor for area

---

4. Actual lesion area was determined by multiplying the surface area obtained in Step 2 with the minification factor for area obtained in Step 3.

   [Surface Area (sq.mm)] x [Minification factor] = Actual Lesion Area (sq.mm)

---

5. Final volume of lesion was determined by multiplying the actual lesion area obtained in Step 4 with the thickness of the CT slices on the image.

   [Actual Lesion Area (sq.mm)] x [CT image slice thickness (mm)] = Volume of Lesion on CT (cu.mm)

APPENDIX M

DESCRIPTION OF CALCULATION OF LESION VOLUME ON MAGNETIC RESONANCE

APPENDIX M

Description of Calculation of Lesion Volume on Magnetic Resonance

---

1. The total number of .05 inch grid boxes for the subject was determined.

---

2. The total number of .05 inch grid boxes was converted into square millimeters to result in a surface area measurement.

   20 grid boxes = 1 inch
   1 inch = 25.4 millimeters
   25.4 mm x 25.4 mm = 645.16 sq.mm
   20 boxes x 20 boxes = 400 boxes

   (25.4 mm / 20) x (25.4 mm / 20) = (645.16 sq.mm / 400) = 1.6129 sq.mm

   [Total number of boxes] x [1.6129 sq. mm] = Surface Area in sq.mm

---

3. In order to allow comparison of lesion size across images and modalities, all measurements were converted to real size. Thus, to counteract for the reduction in size on the images, a correction factor was determined for each image. This correction factor was called a minification factor and was determined by using the conversion scale provided on each image. This factor was squared in order to use in the calculations which followed.

   [MRI conversion scale measurement (mm)] / [Actual size measurement (mm)] = Minification Factor

   [Minification Factor] x [Minification Factor] = Minification Factor for area

---

4. Actual lesion area was determined by multiplying the surface area obtained in Step 2 with the minification factor for area obtained in Step 3.

   [Surface Area (sq.mm)] x [Minification factor] = Actual Lesion Area (sq.mm)

---

5. Direct volume of lesion was determined by multiplying the actual lesion area obtained in Step 4 with the thickness of the MRI slices on the image.

   [Actual Lesion Area (sq.mm)] x [MRI image slice thickness (mm)] = Volume of Lesion on MRI (cu.mm)

Description of Calculation of Lesion Volume on Magnetic Resonance, Continued

---

6. MRI slices are not contiguous but there is a space between each slice. In order to determine the entire extent of the lesion on MRI, the area of the lesion between slices was estimated. This estimate was determined by averaging the two adjoining surface area measurements.

   The number of .05 inch grid boxes between slices was determined.

---

7. Repeat Step 2 above for number of boxes in Step 6.

---

8. Enter Minification Factor from Step 3 above.

---

9. Multiply Steps 7 and 8.

---

10. Estimated volume of the lesion between slices was determined by multiplying the lesion area obtained in Step 9 with the thickness of the interslice space on the MRI image.

[Actual Lesion Area (sq.mm)] x [MRI image interslice thickness (mm)] = Volume of Lesion on MRI (cu.mm)

---

11. Total volume of the lesion on MRI was determined by adding the actual lesion volume to the estimated lesion volume between slices.

[Actual Lesion Volume (cu.mm)] x [Estimated Lesion Volume (cu.mm)] = Total Volume on MRI (cu.mm)

APPENDIX N

ILLUSTRATION OF CALCULATION OF LESION VOLUME ON COMPUTED TOMOGRAPHY

APPENDIX N

Illustration of Calculation of Lesion Volume on Computed Tomography

1. Total number of .05 inch grid boxes for subject 1	257.75
2. [Total number of boxes] x [1.6129 sq. mm] = Surface Area in sq.mm	
[257.75] x [1.6129 sq.mm] =	415.725mm
3. [MRI conversion scale measurement (50 mm)] / [Actual size measurement (19 mm)] = Minification Factor (2.632)	
[Minification Factor] x [Minification Factor] = Minification Factor for area	
[2.632] x [2.632] =	6.925
4. [Surface Area (sq.mm)] x [Minification factor] = Actual Lesion Area (sq.mm)	
[415.725 (sq.mm)] x [6.925] =	2879.020 sq.mm
5. [Actual Lesion Area (sq.mm)] x [MRI image slice thickness (mm)] = Volume of Lesion on MRI (cu.mm)	
[2879.020 (sq.mm)] x [10.0 (mm)] =	28790.203 cu.mm

APPENDIX O

ILLUSTRATION OF CALCULATION OF LESION VOLUME ON MAGNETIC RESONANCE

APPENDIX O

Illustration of Calculation of Lesion Volume on Magnetic Resonance

1. Total number of .05 inch grid boxes for subject 1	289.25
2. [Total number of boxes] x [1.6129 sq. mm] = Surface Area in sq.mm	
[289.25] x [1.6129 sq.mm] =	466.531 sq.mm
3. [MRI conversion scale measurement (100 mm)] / [Actual size measurement (32.0 mm)] = Minification Factor (3.125)	
[Minification Factor] x [Minification Factor] = Minification Factor for area	
[3.125] x [3.125] =	9.7656
4. [Surface Area (sq.mm)] x [Minification factor] = Actual Lesion Area (sq.mm)	
[466.531 (sq.mm)] x [9.7656] =	4555.958 sq.mm
5. [Actual Lesion Area (sq.mm)] x [MRI image slice thickness (mm)] = Volume of Lesion on MRI (cu.mm)	
[4555.958 (sq.mm)] x [5.0 (mm)] =	22779.79 cu.mm
6. The number of .05 inch grid boxes between slices	189.375
7. [Total number of estimated boxes] x [1.6129 (sq.mm)] = Estimated Surface Area in sq.mm	
[189.375] x [1.6129 (sq.mm)] =	305.443 sq.mm
8. Enter Minification Factor from Step 3 above	9.7656
9. [Estimated Surface Area (sq.mm)] x [Minification Factor] = Estimated Lesion Area (sq.mm)	
[305.443 (sq.mm)] x [9.7656 (sq.mm)] =	2982.834
10. [Estimated Lesion Area (sq.mm)] x [MRI image interslice thickness (mm)] = Estimated Volume of interspace lesion on MRI (cu.mm)	
[2982.834 (sq.mm)] x [2.5 (mm)] =	7457.084 cu.mm
11. [Actual Lesion Volume (cu.mm)] x [Estimated Lesion Volume (cu.mm)] = Total Volume on MRI (cu.mm)	
[22779.79 (cu.mm)] x [7457.084 (cu.mm)] =	30236.874 cu.mm

APPENDIX P

RADIOLOGISTS' REPLICATED MEASUREMENTS OF SURFACE AREA OF TARGET LESION ON CT AND MRI

APPENDIX P

Radiologists' Replicated Measurements of Surface Area (number of .05 inch grid boxes) of Target Lesion on CT and MRI

		Surface Area of Lesion			
		Computed Tomography		Magnetic Resonance	
Subject	Radiologist	Judge 1	Judge 2	Judge 1	Judge 2
1					
	A	280	277	330	311
	B	296	292	261	255
	C	225	218	216	217
1 (Replicated Measurement)					
	A	314	309	383	374
	B	413	405	214	216
	C	179	185	279	285
2					
	A	1	1	5	4
	B	3	2	4	3
	C	1	1	2	2
2 (Replicated Measurement)					
	A	5	4	5	5
	B	2	2	3	3
	C	1	1	1	1

APPENDIX Q

JUDGES' REPLICATED CALCULATIONS OF SURFACE AREA OF TARGET LESION ON CT AND MRI

APPENDIX Q

Judges' Replicated Calculations of Surface Area
(number of .05 inch grid boxes) of Target Lesion on CT and MRI

		Surface Area of Lesion			
		Computed Tomography		Magnetic Resonance	
Subject	Radiologist	Judge 1	Judge 2	Judge 1	Judge 2
1					
	A	280	277	330	311
	B	296	292	261	255
	C	225	218	216	217
1 (Replicated measurement)					
	A	278	282	320	325
	B	290	299	247	259
	C	217	227	200	223
5					
	A	8	8	7	8
	B	7	6	9	7
	C	7	7	7	6
5 (Replicated measurement)					
	A	8	8	7	8
	B	7	7	8	7
	C	7	7	7	6

APPENDIX R

DISTRIBUTION OF THREE RADIOLOGISTS' RESPONSES WITH RESPECT TO ANATOMY OF LESIONS SEEN ON COMPUTED TOMOGRAPHY SCANS

APPENDIX R

Distribution of Three Radiologists' Responses with Respect to Anatomy of Lesions Seen on Computed Tomography Scans

			Subjects										Totals
			1	2	3	4	5	6	7	8	9	10	
Hemisphere Lobes	Frontal	Cortex				3				1			4
		White			1	3				2			6
	Parietal	Cortex	1			1		3		1		2	8
		White	1	1	3	1		3		1		2	12
	Occipital	Cortex	3					1	3		3		10
		White	3					1	3		3		10
	Temporal	Cortex	3			3		2		3		2	13
		White	3			3		2		3		3	14
	Insula	Anterior								3			3
		Posterior								3			3
Deep Structures	External Capsule											1	1
	Claustrum												0
	Extreme Capsule												0
	Caudate	Head				3	3			1			7
		Body											0
	Thalamus	Anterior											0
		Pulvinar											0
	Globus Pallidus			1						1			2
	Putamen	Anterior								2			2
		Posterior								1			1
	Lenticular Nucleus					3						1	4
	Internal Capsule	Anterior				2				1			3
		Posterior		1		1							2
	Amygdala												0
	Corpus Callosum	Splenium											0

Total: 105

APPENDIX S

DISTRIBUTION OF THREE RADIOLOGISTS' RESPONSES WITH RESPECT TO ANATOMY OF LESIONS SEEN ON MAGNETIC RESONANCE IMAGING SCANS

APPENDIX S

Distribution of Three Radiologists' Responses with Respect to Anatomy of Lesions Seen on Magnetic Resonance Imaging Scans

			Subjects										Totals
			1	2	3	4	5	6	7	8	9	10	
Hemisphere Lobes	Frontal	Cortex				2				1		1	4
		White				2				2		2	6
	Parietal	Cortex	1			2		2		1		1	7
		White	1		3	2		2		1		2	11
	Occipital	Cortex	3					3	3		3		12
		White	3					3	3		3		12
	Temporal	Cortex	3			3		1		2		2	11
		White	3			3		1		3		2	12
	Insula	Anterior				2				3		2	7
		Posterior	1			2				3		2	8
Deep Structures	External Capsule					1		1		2		1	5
	Claustrum					1		1		1		1	4
	Extreme Capsule					1		1		1		2	5
	Caudate	Head				1	3					2	6
		Body				2						1	3
	Thalamus	Anterior		2									2
		Pulvinar	1										1
	Globus Pallidus			1		2				1		1	5
	Putamen	Anterior				3				2		2	7
		Posterior		1		3				1			5
	Lenticular Nucleus												0
	Internal Capsule	Anterior				1						1	2
		Posterior		1									1
	Amygdala											1	1
	Corpus Callosum	Splenium							1				1
												Total:	138

APPENDIX T

LOCALIZATION OF TARGET LESIONS ON COMPUTED TOMOGRAPHY AND MAGNETIC RESONANCE AS REPORTED BY RADIOLOGIST A

APPENDIX T

Localization of Target Lesions on Computed Tomography and Magnetic Resonance as Reported by Radiologist A

	Subjects									
	1	2	3	4	5	6	7	8	9	10
Frontal Lobe										
Cortical gray matter				CT						
Subcortical white matter				CT						
Parietal Lobe										
Cortical gray matter				CT/MR		CT				
Subcortical white matter		CT	CT/MR	CT/MR		CT				
Occipital Lobe										
Cortical gray matter	CT/MR					CT/MR	CT/MR		CT/MR	
Subcortical white matter	CT/MR					CT/MR	CT/MR		CT/MR	
Temporal Lobe										
Cortical gray matter	CT/MR			CT/MR				CT/MR		MR
Subcortical white matter	CT/MR			CT/MR				CT/MR		CT
Insular gray matter:										
anterior				MR				CT/MR		
posterior				MR				CT/MR		
Subcortical Structures										
Caudate:										
head				CT/MR	CT/MR			CT		
body										MR
Thalamus:										
anterior/lateral		MR								
pulvinar										
Globus Pallidus				MR				MR		MR
Putamen:										
anterior				MR				CT/MR		MR
posterior				MR				CT/MR		
(Lenticular Nucleus)				CT						
Internal Capsule:										
anterior limb				CT				CT		
posterior limb										
External Capsule								MR		
Claustrum										
Extreme Capsule										
Amygdala										MR
Corpus Callosum:										
splenium										
Total: CT/MRI	4/4	1/1	1/1	9/10	1/1	4/2	2/2	8/8	2/2	1/5

APPENDIX U

LOCALIZATION OF TARGET LESIONS ON COMPUTED TOMOGRAPHY AND MAGNETIC RESONANCE AS REPORTED BY RADIOLOGIST B

APPENDIX U

Localization of Target Lesions on Computed Tomography and Magnetic Resonance as Reported by Radiologist B

	Subjects									
	1	2	3	4	5	6	7	8	9	10
Frontal Lobe										
Cortical gray matter				CT/MR				CT/MR		MR
Subcortical white matter				CT/MR				CT/MR		MR
Parietal Lobe										
Cortical gray matter	CT/MR			MR		CT/MR		CT/MR		CT/MR
Subcortical white matter	CT/MR		CT/MR	MR		CT/MR		CT/MR		CT/MR
Occipital Lobe										
Cortical gray matter	CT/MR					MR	CT/MR		CT/MR	
Subcortical white matter	CT/MR					MR	CT/MR		CT/MR	
Temporal Lobe										
Cortical gray matter	CT/MR			CT/MR		CT/MR		CT/MR		CT/MR
Subcortical white matter	CT/MR			CT/MR		CT/MR		CT/MR		CT/MR
Insular gray matter:										
anterior				MR				CT/MR		MR
posterior	MR			MR				CT/MR		MR
Subcortical Structures										
Caudate:										
head				CT	CT/MR					MR
body				MR						
Thalamus:										
anterior/lateral		MR								
pulvinar										
Globus Pallidus		CT/MR		MR						
Putamen:										
anterior				MR						
posterior				MR						
(Lenticular Nucleus)				CT						
Internal Capsule:										
anterior limb										
posterior limb		MR								
External Capsule				MR		MR		MR		MR
Claustrum				MR		MR		MR		MR
Extreme Capsule				MR		MR		MR		MR
Amygdala										
Corpus Callosum:										
splenium							MR			
Total: CT/MRI	6/7	1/3	1/1	6/15	1/1	4/9	2/3	8/11	2/2	4/12

APPENDIX V

LOCALIZATION OF TARGET LESIONS ON COMPUTED TOMOGRAPHY AND MAGNETIC RESONANCE AS REPORTED BY RADIOLOGIST C

APPENDIX V

Localization of Target Lesions on Computed Tomography and Magnetic Resonance as Reported by Radiologist C

	Subjects									
	1	2	3	4	5	6	7	8	9	10
Frontal Lobe										
Cortical gray matter				CT/MR						
Subcortical white matter			CT	CT/MR				CT/MR		MR
Parietal Lobe										
Cortical gray matter						CT/MR				CT
Subcortical white matter			CT/MR			CT/MR				CT/MR
Occipital Lobe										
Cortical gray matter	CT/MR					MR	CT/MR		CT/MR	
Subcortical white matter	CT/MR					MR	CT/MR		CT/MR	
Temporal Lobe										
Cortical gray matter	CT/MR			CT/MR		CT		CT		CT
Subcortical white matter	CT/MR			CT/MR		CT		CT/MR		CT/MR
Insular gray matter:										
anterior								CT/MR		MR
posterior								CT/MR		MR
Subcortical Structures										
Caudate:										
head				CT	CT/MR					MR
body				MR						
Thalamus:										
anterior/lateral										
pulvinar	MR									
Globus Pallidus								CT		
Putamen:										
anterior				MR				CT/MR		MR
posterior		MR		MR						
(Lenticular Nucleus)				CT						CT
Internal Capsule:										
anterior limb				CT/MR						MR
posterior limb		CT		CT						
External Capsule										CT
Claustrum										
Extreme Capsule										MR
Amygdala										
Corpus Callosum:										
splenium										
Total: CT/MRI	4/5	1/1	2/1	8/8	1/1*	4/4	2/2*	7/5	2/2*	6/9

APPENDIX W

REPEATED OBSERVATIONS OF LESION LOCATION FOR TWO SUBJECTS ON COMPUTED TOMOGRAPHY AND MAGNETIC RESONANCE BY RADIOLOGIST A

APPENDIX W

Repeated Observations of Lesion Location for Two Subjects on Computed Tomography and Magnetic Resonance by Radiologist A

	Subjects					
	1	2		1 (Repeated)	2 (Repeated)	
Frontal Lobe						
Cortical gray matter						
Subcortical white matter						
Parietal Lobe						
Cortical gray matter						
Subcortical white matter		CT			CT/MR	
Occipital Lobe						
Cortical gray matter	CT/MR			CT/MR		
Subcortical white matter	CT/MR			CT/MR		
Temporal Lobe						
Cortical gray matter	CT/MR			CT/MR		
Subcortical white matter	CT/MR			CT/MR		
Insular gray matter:						
anterior						
posterior						
Subcortical Structures						
Caudate:						
head						
body						
Thalamus:						
anterior/lateral		MR				
pulvinar						
Globus Pallidus						
Putamen:						
anterior						
posterior						
(Lenticular Nucleus)						
Internal Capsule:						
anterior limb						
posterior limb						
External Capsule						
Claustrum						
Extreme Capsule						
Amygdala				MR		
Corpus Callosum:						
splenium						
Total: CT/MRI	4/4	1/1		4/5	1/1	

APPENDIX X

REPEATED OBSERVATIONS OF LESION LOCATION FOR TWO SUBJECTS ON COMPUTED TOMOGRAPHY AND MAGNETIC RESONANCE BY RADIOLOGIST B

APPENDIX X

Repeated Observations of Lesion Location for Two Subjects on Computed Tomography and Magnetic Resonance by Radiologist B

	Subjects					
	1	2		1 (Repeated)	2 (Repeated)	
Frontal Lobe						
Cortical gray matter						
Subcortical white matter						
Parietal Lobe						
Cortical gray matter	CT/MR			CT		
Subcortical white matter	CT/MR			CT	MR	
Occipital Lobe						
Cortical gray matter	CT/MR			CT/MR		
Subcortical white matter	CT/MR			CT/MR		
Temporal Lobe						
Cortical gray matter	CT/MR			CT/MR		
Subcortical white matter	CT/MR			CT/MR		
Insular gray matter:						
anterior						
posterior	MR					
Subcortical Structures						
Caudate:						
head						
body						
Thalamus:						
anterior/lateral		MR			CT/MR	
pulvinar						
Globus Pallidus		CT/MR				
Putamen:						
anterior						
posterior						
(Lenticular Nucleus)						
Internal Capsule:						
anterior limb						
posterior limb		MR				
External Capsule						
Claustrum						
Extreme Capsule						
Amygdala						
Corpus Callosum:						
splenium						
Total: CT/MRI	6/7	1/3		6/4	1/2	

APPENDIX Y

REPEATED OBSERVATIONS OF LESION LOCATION FOR TWO SUBJECTS ON COMPUTED TOMOGRAPHY AND MAGNETIC RESONANCE BY RADIOLOGIST C

APPENDIX Y

Repeated Observations of Lesion Location for Two Subjects on Computed Tomography and Magnetic Resonance by Radiologist C

	Subjects					
	1	2		1 (Repeated)	2 (Repeated)	
Frontal Lobe						
Cortical gray matter						
Subcortical white matter						
Parietal Lobe						
Cortical gray matter						
Subcortical white matter						
Occipital Lobe						
Cortical gray matter	CT/MR			CT/MR		
Subcortical white matter	CT/MR			CT/MR		
Temporal Lobe						
Cortical gray matter	CT/MR			CT		
Subcortical white matter	CT/MR			CT/MR	CT	
Insular gray matter:						
anterior				MR		
posterior						
Subcortical Structures						
Caudate:						
head						
body						
Thalamus:						
anterior/lateral						
pulvinar	MR					
Globus Pallidus						
Putamen:						
anterior						
posterior		MR				
(Lenticular Nucleus)						
Internal Capsule:						
anterior limb						
posterior limb		CT			CT/MR	
External Capsule						
Claustrum						
Extreme Capsule						
Amygdala						
Corpus Callosum:						
splenium						
Total: CT/MRI	4/5	1/1		4/4	2/1	

LIST OF REFERENCES

LIST OF REFERENCES

Adams, R.D. & Sidman, R.L. (1968). Introduction to neuropathology. New York: McGraw-Hill Book Company.

Agnoli, A. & Feliciani, M. (1987). Nuclear magnetic resonance imaging in the aging brain. Gerontology, 33, 247-252.

Albert, M.L. & Helm-Estabrooks, N. (1988). Diagnosis and treatment of aphasia. Journal of the American Medical Association, 259, 1043-1047.

Alexander, Naeser, & Palumbo. (1987). Correlations of subcortical CT lesion sites and aphasia profiles. Brain, 110, 961-991.

Awad, I.A., Spetzler, R.F., Hodak, J.A., Awad, C.A., & Carey, R. (1986). Incidental subcortical lesions identified on magnetic resonance imaging in the elderly. I. Correlation with age and cerebrovascular risk factors. Stroke, 17, 1084-1089.

Basso, A., Bracchi, M., Capitani, E., Laiacona, M., & Zanobio, M.E. (1987). Age and evolution of language area functions, a study on adult stroke patients. Cortex, 23, 475-483.

Basso, A., Capitani, E., Laiacona, M., & Zanobio, M.E. (1985). Crossed aphasia: One or more syndromes? Cortex, 21, 25-45.

Basso, A., Lecours, A.R., Moraschini, S., & Vanier, M. (1985). Anatomoclinical correlations of the aphasias as defined through computerized tomography: Exceptions. Brain and Language, 26, 201-229.

Benson, D. F. (1967). Fluency in aphasia: Correlation with radioactive scan localization. Cortex, 3, 373-394.

Benson, D. F. & Patten, D. H. (1967). The use of radioactive isotopes in the localization of aphasia-producing lesions. Cortex, 3, 258-271.

Benton, A. L. (1964). Contributions to aphasia before Broca. Cortex, 1, 314-327.

Benton, A. L. & Joynt, R. J. (1960). Early descriptions of aphasia. Archives of Neurology, 3, 109-126.

Berker, E. A., Berker, A. H., & Smith, A. (1986). Translation of

Broca's 1865 report: Localization of speech in the third left frontal convolution. Archives of Neurology, 43, 1065-1072.

Bories, J., Derhy, S., & Chiras, J. (1985). CT in hemispheric ischaemic attacks. Neuroradiology, 27, 468-483.

Bradley, W.G. (1986). Magnetic resonance imaging of the posterior fossa and brainstem. Seminars in Neurology, 6, 8-16.

Bradley, W.G. (1987). Pathophysiologic correlates of signal alterations. In M. Brant-Zawadzki & D. Norman (Eds.), Magnetic resonance imaging of the central nervous system. (pp. 23-42). New York: Raven Press.

Braffman, B.H., Zimmerman, R.A., Trojanowski, J.Q., Gonatas, N.K., Hickey, W.F., & Schlaepfer, W.W. (1988). Brain MR: Pathologic correlation with gross and histopathology. American Journal of Radiology, 151, 559-566.

Brant-Zawadzki, M. (1988). MR imaging of the brain. Radiology, 166, 1-10.

Brant-Zawadzki, M., Davis, P.L., Crooks, L.E., Mills, C.M., Norman, D., Newton, T.H., Sheldon, P., & Kaufman, L. (1983). NMR demonstration of cerebral abnormalities: Comparison with CT. American Journal of Roentgenology, 140, 847-854.

Brant-Zawadzki, M. & Kucharczyk, W. (1987). Vascular disease: Ischemia. In M. Brant-Zawadzki & D. Norman (Eds.), Magnetic resonance imaging of the central nervous system. New York: Raven Press.

Brant-Zawadzki, M., Solomon, M., Newton, T.H., Weinstein, P., Schmidley, J., & Norman, D. (1985). Basic principles of magnetic resonance imaging in cerebral ischemia and initial clinical experience. Neuroradiology, 27, 517-520.

Brown, J.J., Hesselink, J.R., & Rothrock, J.F. (1988). MR and CT of lacunar infarcts. American Journal of Neuroradiology, 9, 477-482.

Bruning, J.L. & Kintz, B.L. (1968). Computational handbook of statistics. Glenview, Ill.: Scott, Roresman and Company.

Brunner, R. J., Kornhuber, H. H., Seemuller, E., Suger, G., & Wallesch, C. W. (1982). Basal ganglia participation in language pathology. Brain and Language, 16, 281-299.

Bydder, G.M. (1984). Magnetic resonance imaging of the brain. Radiologic Clinics of North America, 22, 779-793.

Bydder, G.M. & Steiner, R.E. (1982). NMR imaging of the brain. Neuroradiology, 23, 231-240.

Bydder, G.M., Steiner, R.E., Young, I.R., Hall, A.S., Thomas, D.J., Marshall, J., Pallis, C.A., & Legg, N.J. (1982). Clinical NMR imaging of the brain: 140 cases. American Journal of Radiology, 139, 215-236.

Caplan, L.R. & DeWitt, L.D. (1988). Determining the cause of aphasia. MRI Decisions, 2, 2-13.

Carroll, Q.B. (1985). Fuchs's principles of radiographic exposure, processing and quality control. Springfield, Ill.: Charles C. Thomas.

Cooper, L.S., Chalmers, T.C., McCally, M., Berrier, J., & Sacks, H.S. (1988). The poor quality of evaluations of magnetic resonance imaging. Journal of the American Medical Association, 259, 3277-3280.

Crooks, L.E., Mills, C.M., Davis, P.L., Brant-Zawadski, M., Hoenninger, J., Arakawa, M., Watts, J., & Kaufman, L. (1982). Visualization of cerebral and vascular abnormalities by NMR imaging. The effects of imaging parameters on contrast. Radiology, 144, 843-852.

Damadian, R. (1971). Tumor detection by nuclear magnetic resonance. Science, 171, 1151-1153.

Damasio, A. R., Damasio, H., Rizzo, M., Varney, N., & Gersh, F. (1982). Aphasia with nonhemorrhagic lesions in the basal ganglia and internal capsule. Archives of Neurology, 39, 15-20.

De Groot, J. (1984). Correlative neuroanatomy of computed tomography and magnetic resonance imaging. Philadelphia: Lea & Febiger.

Demeurisse, G., Capon, A., & Verhas, M. (1985). Prognostic value of computed tomography in aphasic stroke patients. European Neurology, 24, 134-139.

DeWitt, L.D., Buonanno, F.S., Kistler, J.P., Brady, T.J., Pykett, I.L., Goldman, M.R., & Davis, K.R. (1984). Nuclear magnetic resonance imaging in evaluation of clinical stroke syndromes. Annals of Neurology, 16, 535-545.

DeWitt, L.D., Grek, A., Buonanno, F., Levine, D.N., & Kistler, J.P. (1985). MRI and the study of aphasia. Neurology, 35, 861-865.

Duverger, D. & MacKenzie, E.T. (1988). The quantification of cerebral infarction following focal ischemia in the rat: Influence of strain, arterial pressure, blood glucose concentration, and age. Journal of Cerebral Blood Flow and Metabolism, 8, 449-461.

Eisenson, J. (1947). Aphasics: Observations and tentative conclusions. Journal of Speech Disorders, 12, 290-292.

Eisenson, J. (1949). Prognostic factors related to language rehabilitation in aphasic patients. Journal of Speech and Hearing Disorders, 14, 262-264.

Elster, A.D. (1986). Magnetic resonance imaging: A reference guide and atlas. Philadelphia: J.B. Lippincott Company.

Fazekas, F., Niederkorn, K., Schmidt, R., Offenbacher, H., Horner, S., Bertha, G., & Lechner, H. (1988). White matter signal abnormalities in normal individuals: Correlation with carotid ultrasonography, cerebral blood flow measurements, and cerebrovascular risk factors. Stroke, 19, 1285-1288.

Fisher, C.M. (1982). Lacunar strokes and infarcts: A review. Neurology, 32, 871-876.

Freedman, L.S. (1987). Evaluating and comparing imaging techniques: a review and classification of study designs. The British Journal of Radiology, 60, 1071-1081.

Friedman, P.J. (1988). The early evaluations of MR imaging. American Journal of Radiology, 151, 860-861.

Fromm, D., Holland, A.L., Swindell, C.S., & Reinmuth, O.M. (1985). Various consequences of subcortical stroke: Prospective study of 16 consecutive cases. Archives of Neurology, 42, 943-950.

Gademann, G. (1984). NMR-tomography of the normal brain. Berlin: Springer-Verlag.

General Electric, (1984). Magnetic Resonance System. Milwaukee: General Electric Co.

Goldberg, H.I. (1983). Stroke. In S.H. Lee & K.C.V.G. Rao (Eds.), Cranial computed tomography (pp. 583-658). New York: McGraw-Hill Book Company.

Goodglass, H. & Kaplan, E. (1972). The assessment of aphasia and related disorders. Philadelphia: Lea & Febiger.

Goodglass, H. & Kaplan, E. (1984). The assessment of aphasia and related disorders. Philadelphia: Lea & Febiger.

Grubbs, F.E. & Beck, G. (1972). Extension of sample sizes and percentage points for significance tests of outlying observations. Technometrics, 14, 847-854.

Hanaway, J., Scott, W.R., & Strother, C.M. (1980). Atlas of the human brain and the orbit for computed tomography. St. Louis: Warren H. Green, Inc.

Haughton, V.M., Rimm, A.A., Sobocinski, K.A., Papke, R.A., Daniels, D.L., Williams, A.L., Lynch, R., & Levine, R. (1986). A blinded

clinical comparison of MR imaging and CT in neuroradiology. Radiology, 160, 751-755.

Hayward, R.W., Naeser, M.A., & Zatz, L.M. (1977). Cranial computed tomography in aphasia. Radiology, 123, 653-660.

Jones, J.P., Partain, C.L., Mitchell, M.R., Patton, J.A., Stephens, W.H., Price, R.R., Kulkarni, M.V., & James, A.E. (1985). Principles of magnetic resonance. In H. Kressel (Ed.), Magnetic resonance annual, (pp.71-112).

Kachigan, S.K. (1986). Statistical analysis: An interdisciplinary introduction to univariate & multivariate methods. New York: Radius Press.

Katz, M. (1984). Principles and techniques of image reconstruction with CT. In L. Weisberg, C. Nice, & M. Katz (Eds.). Cerebral computed tomography: A text atlas. Philadelphia: W.B. Saunders Company.

Kean, D. & Smith, M. (1986). Magnetic resonance imaging: Principles and applications. Baltimore: Williams & Wilkins.

Kertesz, A., Black, S.E., Nicholson, L., & Carr, T. (1987). The sensitivity and specificity of MRI in stroke. Neurology, 37, 1580-1585.

Kertesz, A., Black, S.E., Tokar, G., Benke, T., Carr, T., Nicholson, L. (1988). Periventricular and subcortical hyperintensities on magnetic resonance imaging: Rims, caps, and unidentified bright objects. Archives of Neurology, 45, 404-408.

Kertesz, A., Harlock, W., & Coates, R. (1979). Computer tomographic localization, lesion size and prognosis in aphasia and nonverbal impairment. Brain and Language, 8, 34-50.

Kinkel, P.R., Kinkel, W.R., & Jacobs, L. (1986). Nuclear magnetic resonance imaging in patients with stroke. Seminars in Neurology, 6, 43-52.

Kistler, J.P., Buonanno, F.S., Roh, J.K., & Davis, K.R. (1986). Diagnostic approaches to cerebrovascular disease. Seminars in Neurology, 6, 254-261.

Kluger, A., Gianutsos, J., deLeon, M.J., & George, A.E. (1988). Significance of age-related white matter lesions. Stroke, 19, 1054-1055.

Knopman, D.S. & Rubens, A.B. (1986). The validity of computed tomographic scan findings for the localization of cerebral functions. Archives of Neurology, 43, 328-332.

Koehler, P.R., Anderson, R.E., & Baxter, B. (1979). The effect of

computed tomography viewer controls on anatomical measurements. Radiology, 130, 189-194.

Kundel, H.L. & LaFollette, P.S. (1972). Visual search patterns and experience with radiological images. Radiology, 103, 523-528.

Laakman, R.W., Kaufman, B., Han, J.S., Nelson, A.D., Clampitt, M., O'Block, A.M., Haaga, J.R., & Alfidi, R.J. (1985). MR imaging in patients with metallic implants. Radiology, 157, 711-714.

Lechner, H., Schmidt, R., Bertha, G., Justich, E., Offenbacher, H., & Schneider, G. (1988). Nuclear magnetic resonance image white matter lesions and risk factors for stroke in normal individuals. Stroke, 19, 263-265.

Lee, D., Fox, A., Vinuela, F., Pelz, D., Lau, C., Donald, A., & Merskey, H. (1987). Interobserver variation in computed tomography of the brain. Archives of Neurology, 44, 30-31.

Lauterbur, P.C. (1973). Image formation by induced local interactions: Examples employing nuclear magnetic resonance. Nature, 242, 190-191.

Martin, J.H. & Brust, J.C.M. (1985). Imaging the living brain. In E.R. Kandel & J.H. Schwartz (Eds.), Principles of neural science (pp.259-283). New York: Elsevier.

Mazzocchi, F. & Vignolo, L.A. (1979). Localisation of lesions in aphasia: Clinical-CT scan correlations in stroke patients. Cortex, 15, 627-653.

Mohr, J.P. (1982). Lacunes. Stroke, 13, 3-11.

Mohr, J.P., Pessin, M.S., Finkelstein, S., Funkenstein, H.H., Duncan, G.W., & Davis, K.R. (1978). Broca aphasia: Pathologic and clinical. Neurology, 28, 311-324.

Moseley, I. (1988). Acute disturbances of cerebral function: Stroke and cerebrovascular disease. In I. Moseley (Ed.). Magnetic resonance imaging in diseases of the nervous system. Oxford: Blackwell Scientific Publications.

Murdoch, B.E. (1988). Computerized tomographic scanning: its contributions to the understanding of the neuroanatomical basis of aphasia. Aphasiology, 2, 437-462.

Murdoch, B.E., Afford, R.J., Ling, A.R., & Ganguley, B. (1986). Acute computerized tomographic scans: Their value in the localization of lesions and as prognostic indicators in aphasia. Journal of Communication Disorders, 19, 311-345.

Naeser, M. A. (1983). CT scan lesion size and lesion locus in cortical and subcortical aphasias. In A. Kertesz (Ed.), Localization

in neuropsychology (pp. 63-119). New York: Academic Press.

Naeser, M.A. (1985). Quantitative approaches to computerized tomography in behavioral neurology. In M.M. Mesulam (Ed.), Principles of behavioral neurology (pp. 363-383). Philadelphia: F.A. Davis Co.

Naeser, M.A. (1988). Some effects of subcortical white matter lesions on language behaviour in aphasia. Aphasiology, 2, 363-368.

Naeser, M.A., Alexander, M.P., Helm-Estabrooks, N., Levine, H.L., Laughlin, S.A., & Geschwind, N. (1982). Aphasia with predominantly subcortical lesion sites: Description of three capsular/putaminal aphasia syndromes. Archives of Neurology, 39, 2-14.

Naeser, M.A., Gaddie, A., Palumbo, C.L. & Stiassny-Eder, D. (1989). Late recovery of auditory comprehension in global aphasia: improved recovery observed with subcortical temporal isthmus lesion vs. Wernicke's cortical area lesion. Manuscript submitted for publication.

Naeser, M.A. & Hayward, R.W. (1978). Lesion localization in aphasia with cranial computed tomography and the Boston Diagnostic Aphasia Exam. Neurology, 28, 545-551.

Naeser, M.A., Hayward, R.W., Laughlin, S.A., & Zatz, L.M. (1981). Quantitative CT scan studies in aphasia. Brain and Language, 12, 140-164.

Naeser, M. A., Helm-Estabrooks, N., Haas, G., Auerbach, S., & Srinivasan, M. (1987). Relationship between lesion extent in Wernicke's area on computed tomographic scan and predicting recovery of comprehension in Wernicke's aphasia. Archives of Neurology, 44, 73-82.

Naeser, M.A., Palumbo, C.L., Helm-Estabrooks, N., Stiassny-Eder, D., & Albert, M.L. (1989). Severe non-fluency in aphasia: role of the medial subcallosal fasciculus plus other white matter pathways in recovery of spontaneous speech. Brain, 112, 1-38.

Naruse, S. & Hirakawa, K. (1986). Brain edema studied by magnetic resonance. Seminars in Neurology, 6, 53-64.

Oldendorf, W.H. (1985). Principles of imaging structure by NMR. In L. Sokoloff (Ed.), Brain Imaging and Brain Function (pp. 245-257). New York: Raven Press.

Pavlicek, W. (1988). Safety considerations. In D.D. Stark & W.G. Bradley (Eds.). Magnetic resonance imaging (pp.244-257). St Louis: C.V. Mosby Co.

Pavlicek, W., Geisinger, M., Castle, L., Borkowski, B.P., Meaney, T.F., Bream, B.L., & Gallagher, J.H. (1983). The effects of nuclear magnetic resonance on patients with cardiac pacemakers. Radiology,

147, 149-153.

Peach, R. K. & Tonkovich, J. D. (1983). Subcortical aphasia: A report of three cases. In R. H. Brookshire (Ed.), Clinical Aphasiology Conference Proceedings (pp. 244-251). Minneapolis: BRK Publishers.

Penfield, W. & Roberts, L. (1959). Speech and brain-mechanisms. Princeton: Princeton University Press.

Pieniadz, J.M., Naeser, M.A., Koff, E., & Levine, H.L. (1983). CT scan cerebral hemispheric asymmetry measurements in stroke cases with global aphasia: atypical asymmetries associated with improved recovery. Cortex, 19, 371-391.

Poeck, K., de Bleser, R., & von Keyserlingk, D.G. (1984). Computed tomography localization of standard aphasic syndromes. In F.C. Rose (Ed.), Advances in neurology, Vol. 42: Progress in aphasiology (pp. 71-89). New York: Raven Press.

Poncet, M., Habib, M., & Robillard, A. (1987). Deep left parietal lobe syndrome: conduction aphasia and other neurobehavioral disorders due to a small subcortical lesion. Journal of Neurology, Neurosurgery, and Psychiatry, 50, 709-713.

Posin, J.P., Ortendahl, D.A., Hylton, N.M., Kaufman, L., Watts, J.C., Crooks, L.E., & Mills, C.M. (1985). Variable magnetic resonance imaging parameters: effect on detection and characterization of lesions. Radiology, 155, 719-725.

Potchen, E.J. (1975). Study on the use of diagnostic radiology. In E.J. Potchen (Ed.), Current concepts in radiology (pp. 18-30). St. Louis: C.V. Mosby Company.

Pykett, I.L., Buonanno, F.S., Brady, T.J., & Kistler, J.P. (1983). True three-dimensional nuclear magnetic resonance neuro-imaging in ischemic stroke: Correlation of NMR, x-ray CT and pathology. Stroke, 14, 173-177.

Reid, A. C., Teasdale, G. M., Matheson, M. S., & Teasdale, E. M. (1981). Serial ventricular volume measurements: further insights into the aetiology and pathogenesis of benign intracranial hypertension. Journal of Neurology, Neurosurgery, and Psychiatry, 44, 636-640.

Rothrock, J.F., Lyden, P.D., Hesselink, J.R., Brown, J.J., & Healy, M.E. (1987). Stroke, 18, 781-786.

Rowland, L.P. (1985). Blood-brain barrier, cerebrospinal fluid, brain edema, and hydrocephalus. In E.R. Kandel & J.H. Schwartz (Eds.), Principles of neural science (pp. 837-844). New York: Elsevier.

Sarpel, G., Chaudry, F., & Hindo, W. (1987). Magnetic resonance imaging of periventricular hyperintensity in a veterans administration hospital population. Archives of Neurology, 44, 725-728.

Seeram, E. (1982). Computed tomography technology. Philadelphia: W.B. Saunders Company.

Selnes, O. A., Knopman, D. S., Niccum, N., Rubens, A. B., & Larson, D. (1983). Computed tomographic scan correlates of auditory comprehension deficits in aphasia: A prospective recovery study. Annals of Neurology, 13, 558-566.

Selnes, O.A., Niccum, N., Knopman, D.S., & Rubens, A.B. (1984). Recovery of single word comprehension: CT scan correlates. Brain and Language, 21, 72-84.

Shinar, D., Gross, C.R., Hier, D.B., Caplan, L.R., Mohr, J.P., Price, T.R., Wolf, P.A., Kase, C.S., Fishman, I.G., Barwick, J.A., & Kunitz, S.C. (1987). Interobserver reliability in the interpretation of computed tomographic scans of stroke patients. Archives of Neurology, 44, 149-155.

Sipponen, J.T. (1984). Uses of techniques: Visualization of brain infarction with nuclear magnetic resonance imaging. Neuroradiology, 26, 387-391.

Sipponen, J.T., Kaste, M., Ketonen, L., Sepponen, R., Katevuo, K., & Sivula, A. (1983). Serial nuclear magnetic resonance (NMR) imaging in patients with cerebral infarction. Journal of Computer Assisted Tomography, 7, 585-589.

Steel, R.G.D. & Torrie, J.H. (1980). Principles and procedures of statistics: A biometrical approach. New York: McGraw-Hill Book Company.

Straub, W.H. (1984). Current diagnostic imaging methods: Relative strengths and limitations. In W.H. Straub (Ed.). Manual of diagnostic imaging (pp. 13-16). Boston: Little, Brown and Company.

Tramo, M.J., Baynes, K., & Volpe, B.T. (1988). Impaired syntactic comprehension and production in Brocas aphasia: CT lesion localization and recovery patterns. Neurology, 38, 95-98.

Tranel, D., Biller, J., Damasio, H., Adams, H.P., & Cornell, S.H. (1987). Global aphasia without hemiparesis, Archives of Neurology, 44, 304-308.

Trapnell, D.H. (1967). Principles of X-ray diagnosis. London: Butterworths.

Unger, E., Littlefield, J., & Gado, M. (1988). Water content and water structure in CT and MR signal changes: Possible influence in detection of early stroke. American Journal of Neuroradiology, 9,

687-691.

Ventry, I. M. & Schiavetti, N. (1980). Evaluating research in speech pathology and audiology. New York: John Wiley & Sons.

Vignolo, L.A. (1984). Aphasias associated with computed tomography scan lesions outside Broca's and Wernicke's areas. In F.C. Rose (Ed.), Advances in Neurology Vol. 42 (pp.91-98). New York: Raven Press.

Vignolo, L.A., Boccardi, E., & Caverni, L. (1986). Unexpected CT-Scan findings in global aphasia. Cortex, 22, 55-69.

Villafana, T. (1983). Physics and instrumentation. In S.H. Lee & K.C.V.G. Rao (Eds.), Cranial computed tomography (pp. 1-46). New York: McGraw-Hill Book Company.

Wallesch, C. W., Kornhuber, H. H., Brunner, R. J., Kunz, T., Hollerbach, B., & Suger, G. (1983). Lesions of the basal ganglia, thalamus, and deep white matter: Differential effects on language functions. Brain and Language, 20, 286-304.

Wang, A.M., Lin, J.C.T., & Rumbaugh, C.L. (1988). What is expected of CT in the evaluation of stroke. Neuroradiology, 30, 54-58.

Wehrli, F.W. & Field-Quick, S. (1988). SIGNA Applications Guide. Milwaukee: General Electric Co.

Weisberg, L., Nice, C., & Katz, M. (1984). Cerebral computed tomography: A text atlas. Philadelphia: W.B. Saunders Company.

Williams, F. (1979). Reasoning with statistics. New York: Holt, Rinehart and Winston.

Yarnell, P., Monroe, P., & Sobel, L. (1976). Aphasia outcome in stroke: A clinical neuroradiological correlation. Stroke, 7, 516-522.

Yock, D.H. (1985). Computed tomography of CNS disease: A teaching file. Chicago: Year Book Medical Publishers, Inc.

Zulch, K.-J. (1985). The cerebral infarct: pathology, pathogenesis, and computed tomography. Berlin: Springer-Verlag.